

1 **The slow slip of viscous faults**

2 **Robert C. Viesca¹, Pierre Dublanchet²**

3 ¹Department of Civil and Environmental Engineering, Tufts University, Medford, Massachusetts, USA.

4 ²MINES ParisTech, PSL Research University, Centre de Géosciences, 35 rue Saint-Honoré, 77300

5 Fontainebleau, France.

6 **Key Points:**

- 7 • Continuum models with rate-strengthening faults exhibit diffusive spreading of
8 fault slip and slip rate.
- 9 • Solve for spatiotemporal evolution of slip and self-similar, long-time asymptotic
10 expansion.
- 11 • Log time-dependence of post-seismic surface displacement and linear moment-duration
12 relation emerge without rate- and state-dependent friction.

13 **Abstract**

14 We examine a simple mechanism for the spatio-temporal evolution of transient, slow slip.
 15 We consider the problem of slip on a fault that lies within an elastic continuum and whose
 16 strength is proportional to sliding rate. This rate dependence may correspond to a vis-
 17 cously deforming shear zone or the linearization of a non-linear, rate-dependent fault strength.
 18 We examine the response of such a fault to external forcing, such as local increases in
 19 shear stress or pore fluid pressure. We show that the slip and slip rate are governed by
 20 a type of diffusion equation, the solution of which is found using a Green's function ap-
 21 proach. We derive the long-time, self-similar asymptotic expansion for slip or slip rate,
 22 which depend on both time t and a similarity coordinate $\eta = x/t$, where x denotes fault
 23 position. The similarity coordinate shows a departure from classical diffusion and is owed
 24 to the non-local nature of elastic interaction among points on an interface between elas-
 25 tic half-spaces. We demonstrate the solution and asymptotic analysis of several exam-
 26 ple problems. Following sudden impositions of loading, we show that slip rate ultimately
 27 decays as $1/t$ while spreading proportionally to t , implying both a logarithmic accumu-
 28 lation of displacement as well as a constant moment rate. We discuss the implication for
 29 models of post-seismic slip as well as spontaneously emerging slow slip events.

30 **1 Introduction**

31 A number of observations point towards the slow, stable slip of faults in the pe-
 32 riod intervening earthquakes. These include observations indicating slow slip following
 33 an earthquake—also known as post-seismic slip, or afterslip—and transient events of fault
 34 creep that appear to emerge spontaneously, without a preceding earthquake. Models for
 35 transient episodes of slow slip look to couple fault sliding with elastic or visco-elastic de-
 36 formation of the host rock and incorporate various constitutive descriptions for the fault
 37 shear strength. We outline prior evidence for slow fault slip, a survey of past models for
 38 such behavior, and highlight an outstanding problem whose solution bridges existing gaps
 39 among models and between models and observations.

40 **1.1 Slow slip observations**

41 Early inference of fault creep, including creep transients and post-seismic slip, re-
 42 lied on the measurement of relative displacement of markers at the surface, designed in-
 43 struments, and repeated geodetic surveys [e.g., Steinbrugge *et al.*, 1960; Smith and Wyss,

44 1968; Scholz *et al.*, 1969; Allen *et al.*, 1972; Bucknam, 1978; Evans, 1981; Beavan *et al.*,
45 1984; Williams *et al.*, 1988; Bilham, 1989; Gladwin, 1994; Linde *et al.*, 1996]. However,
46 using surface displacement measurements to discriminate between fault slip or more dis-
47 tributed deformation or using surface offset measurements to discriminate between shal-
48 low or deep sources of relative displacement were not typically possible, or at least at-
49 tempted, owing to the paucity of information or computational resources.

50

51 The increased spatial-temporal resolution of satellite-based geodetic (chiefly, GPS
52 and InSAR) led to more robust inference of aseismic fault slip. Among the earliest ap-
53 plications was for the inference of post-seismic slip. Typically, this inference was based
54 on the goodness of fit of subsurface dislocation models to observed post-seismic surface
55 displacement. Occasionally, in an attempt to discriminate the source of the post-seismic
56 deformation, the goodness of such fits were compared to those with models that alter-
57 natively or additionally included mechanisms for distributed deformation, such as vis-
58 coelastic relaxation of the asthenosphere or poroelastic rebound of the crust. Notable
59 earthquakes from which post-seismic slip has been inferred using such approaches include
60 Landers '92 [Shen *et al.*, 1994; Savage and Svare, 1997]; Japan Trench '94 [Heki *et al.*,
61 1997]; Colima '95 [Azúa *et al.*, 2002]; Kamchatka '97 [Burgmann *et al.*, 2001]; Izmit '99
62 [Reilinger *et al.*, 2000; Çakir *et al.*, 2013]; Chi-Chi '99 [Yu *et al.*, 2003; Hsu *et al.*, 2002,
63 2007]; Denali '02 [Johnson *et al.*, 2009]; Parkfield '04 [Murray and Segall, 2005; Murray
64 and Langbein, 2006; Johnson *et al.*, 2006; Freed, 2007; Barbot *et al.*, 2009; Bruhat *et al.*,
65 2011]; Sumatra '04 [Hashimoto *et al.*, 2006; Paul *et al.*, 2007]; Nias '05 [Hsu *et al.*, 2006];
66 Pisco '07 [Perfettini *et al.*, 2010]; Maule '10 [Bedford *et al.*, 2013]; and Tohoku '11 [Ozawa
67 *et al.*, 2011, 2012].

68

69 Nearly in parallel, aseismic transients not linked to large earthquakes were discov-
70 ered on subduction zones in Japan [Hirose *et al.*, 1999; Hirose and Obara, 2005; Obara
71 and Hirose, 2006; Hirose *et al.*, 2014], Cascadia [Dragert *et al.*, 2001; Miller *et al.*, 2002;
72 Rogers and Dragert, 2003], Guerrero, Mexico [Lowry *et al.*, 2001; Kostoglodov *et al.*, 2003],
73 New Zealand [Douglas *et al.*, 2005; Wallace and Beavan, 2006], Alaska [Ohta *et al.*, 2006;
74 Fu and Freymueller, 2013]; the Caribbean [Outerbridge *et al.*, 2010], as well as several
75 strike-slip faults [e.g., de Michele *et al.*, 2011; Shirzaei and Burgmann, 2013; Jolivet *et*

76 *al.*, 2013; *Rousset et al.*, 2016]. In addition to the geodetic inference of slip, tremor was
77 also observed seismologically, accompanying subduction zone slow slip events [*Obara*, 2002;
78 *Rogers and Dragert*, 2003; *Obara et al.*, 2004; *Shelley et al.*, 2006; *Obara and Hirose*, 2006;
79 *Ito et al.*, 2007]. The tremor is at least partly comprised of small, low frequency earth-
80 quakes with indications that these events occur as the rupture of small asperities driven
81 by aseismic creep of the surrounding fault [*Shelly et al.*, 2006; *Shelly et al.*, 2007; *Ide et*
82 *al.*, 2007; *Rubinstein et al.*, 2007; *Bartlow et al.*, 2011]. Thus, the presence of tremor alone
83 is a potential indication of underlying slow slip, which may be too small or deep to be
84 well resolved geodetically, in both subduction and strike-slip settings [e.g., *Nadeau and*
85 *Dolenc*, 2005; *Gomberg et al.*, 2008; *Shelly and Johnson*, 2011; *Wech et al.*, 2012; *Guil-*
86 *hem and Nadeau*, 2012].

87 1.2 Models for slow slip

88 Following initial observations of unsteady fault creep, modeling efforts looked to-
89 wards continuum models to reproduce surface observations. Models represented fault slip
90 as a dislocation within an elastic medium and transients as phenomena due to propa-
91 gating rupture fronts or emerging from an explicit rate-dependent frictional strength of
92 the fault [e.g., *Savage*, 1971; *Nason and Weertman*, 1973; *Ida*, 1974; *Wesson*, 1988]. How-
93 ever, because of the sparsity of available data with which to discriminate among hypo-
94 thetical model assumptions, these representations may have been before their time.

95

96 An experimental basis for forward models followed laboratory rock friction exper-
97 iments and the subsequent development of a rate-dependent or a rate- and state-dependent
98 constitutive formulation for fault frictional strength [*Dieterich*, 1978, 1979; *Ruina* 1980,
99 1983]. Incorporation of the rate-and-state description into spring-block models yielded
100 a low-parameter model for both slow and fast fault slip defined in terms of frictional prop-
101 erties, a representative elastic stiffness, and a driving force [*Rice and Ruina*, 1983; *Gu*
102 *et al.*, 1984; *Rice and Tse*, 1986; *Scholz*, 1990; *Marone et al.*, 1991; *Ranjith and Rice*, 1999;
103 *Perfettini and Avouac*, 2004; *Helmstetter and Shaw*, 2009]. For instance, the analysis of
104 such a single-degree-of-freedom model provided a simple representation of post-seismic
105 relaxation of fault slip and simple scaling of displacement and its rate with time capa-

106 ble of matching observed displacement time history at points on the surface [e.g., *Scholz*,
107 *Marone et al.*, 1991; *Perfettini and Avouac*, 2004].

108

109 The increased availability of field observations led to a resurgence of continuum for-
110 ward models, capable of matching multiple station observations with a single parame-
111 terized representation of the fault, as well as permitting the emergence of phenomena
112 not possible within single-degree-of-freedom spring-block models. These include mod-
113 els for the afterslip process [e.g., *Linker and Rice*, 1997; *Hearn et al.*, 2002; *Johnson et*
114 *al.*, 2006; *Perfettini and Ampuero*, 2008; *Barbot et al.*, 2009; *Hetland et al.*, 2010] as well
115 as spontaneous aseismic transients [*Liu and Rice*, 2005, 2007; *Rubin*, 2008; *Segall et al.*,
116 2010; *Ando et al.*, 2010, 2012; *Collela*, 2011; *Skarbek et al.*, 2012; *Shibasaki et al.*, 2012;
117 *Liu*, 2014; *Li and Liu*, 2016; *Romanet et al.*, 2018]. Such continuum models have been
118 theoretically demonstrated to exhibit slowly propagating slip-pulse or detachment-front
119 solutions, which provide additional mechanisms to mediate aseismic rupture, though com-
120 parisons with observations are thus far limited [e.g., *Perrin et al.*, 1995; *Garagash*, 2012;
121 *Bar-Sinai et al.*, 2012; *Putelat et al.*, 2016].

122

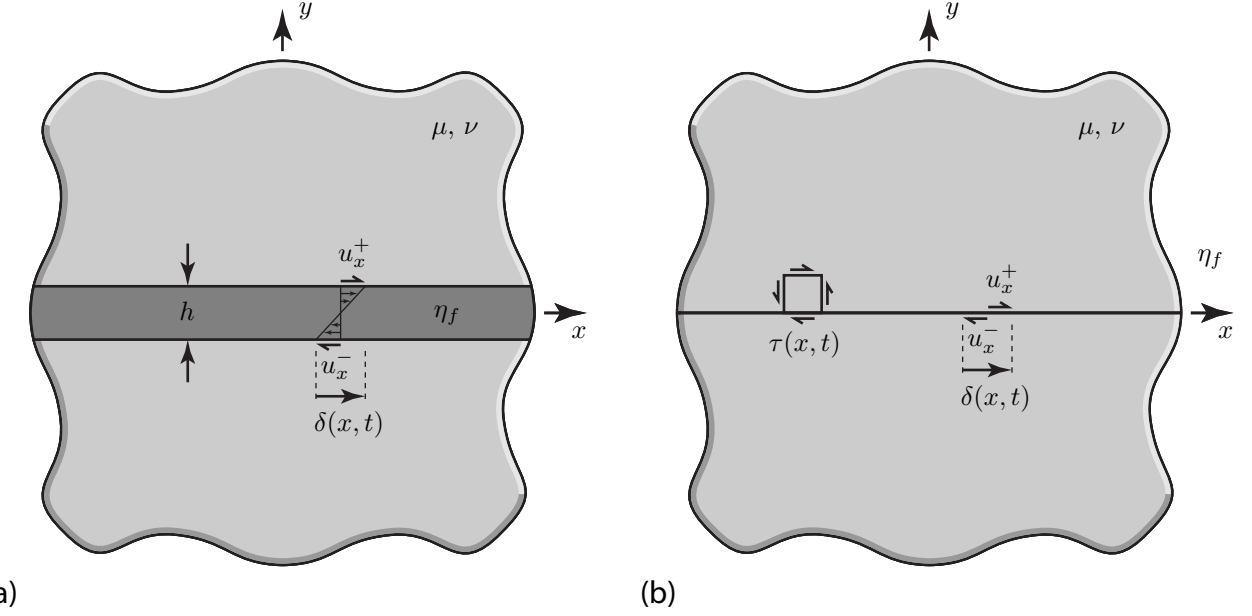
123 In both the continuum and spring-block slider models, rate- and state-dependent
124 friction has remained as the prominent description of fault strength. The constitutive
125 formulation consists of a positive logarithmic dependence on the sliding rate and an ad-
126 ditional dependence on a state variable reflecting the history of sliding. The steady-state
127 behavior is one of a positive (rate-strengthening) or negative (rate-weakening) depen-
128 dence on the logarithm of the sliding rate. Such a state-variable formulation circumvents
129 issues of ill-posedness of continuum models of faults whose strength is solely rate-dependent
130 and a decreasing function of slip rate [e.g., *Rice et al.*, 2001]. However, hypothetical mod-
131 els of stable fault slip allow for a wider range of potential descriptions, including a strictly
132 rate-dependent formulation, which we explore in this work and further motivate in the
133 following section.

134 **1.3 Motivation and outline of current work**

135 We are interested in identifying key signatures of stable fault slip, including the spa-
 136 tiotemporal evolution of fault slip and slip rate in response to finite perturbations. At
 137 an elementary level, this involves the coupling of rate-strengthening fault shear strength
 138 with elastic deformation of the host rock. A rate-strengthening fault can be conceived
 139 to exist due to a number of linear or non-linear physical mechanisms, including rate- and
 140 state-dependent friction or a non-linear viscous response of a shear zone. Each non-linear
 141 formulation has the common feature of being linearizable about a finite or zero slip rate,
 142 tantamount to a linear viscous rheology. Here we consider this linear viscous response
 143 as the simplest rate-strengthening description. In doing so, we will find the universal asymp-
 144 totic behavior for non-linear, rate-strengthening descriptions, the further analysis of which
 145 must be done on a case-by-case basis. Furthermore, in spite of being among the simplest
 146 mechanisms for stable, aseismic slip, the analysis of the mechanical response of faults with
 147 linearly viscous strength has received limited attention, apart from the works of *Ida* [1974],
 148 *Brener and Marchenko* [2002], and *Ando et al.* [2012].

149

150 We take advantage of the linear form of the governing equations to analyze the tran-
 151 sient response of a fault to space- and time-dependent loading. In Section 2 we intro-
 152 duce the equations governing problems in which slip occurs along an interface between
 153 elastic continua and in which the interfacial shear strength is proportional to slip rate.
 154 In Section 3 we introduce a non-dimensionalization and we draw comparisons with an-
 155 other problem: classical diffusion. We find that the two problems have direct analogies
 156 and we denote the problem governing in- or anti-plane viscous slip between elastic half-
 157 spaces as Hilbert diffusion; in Section 4 we provide the Green's function solution to this
 158 problem and use the Green's function approach to solve example initial value problems.
 159 In Section 5, we discuss the self-similar asymptotic expansion of such problems at large
 160 time and, in Section 6, we contrast the long-time behavior of large faults with that of
 161 finite-sized faults and spring-block models. We discuss our results in light of past obser-
 162 vations and models in Section 7.



163 **Figure 1.** Illustration of model geometry and shear zone deformation. (a) A viscous shear
 164 zone of thickness h and viscosity η_f lies between two linear elastic half-spaces of shear modulus μ
 165 and Poisson ratio ν . In-plane deformation of the shear zone is drawn, with the layer undergoing
 166 uniform strain and a relative displacement $\delta = u_x^+ - u_x^-$, where u_x^+ and u_x^- denote the displace-
 167 ment of the top and bottom faces of the shear zone. (b) Over distances much greater than h ,
 168 the problem in (a) appears as two linear-elastic half-spaces in contact undergoing the relative
 169 displacement δ with that motion being resisted by an interfacial shear stress τ .

170 2 Governing equations

171 We consider a fault shear zone to be a layer parallel to the x - z plane with a uni-
 172 form thickness h in the fault-normal coordinate y (Figure 1a). We presume that defor-
 173 mation is either within the x - y plane (in-plane) or in the z -direction alone (anti-plane)
 174 and we denote τ as the stress component σ_{yx} or σ_{yz} within the shear zone for the in- and
 175 anti-plane cases, respectively. We presume inelastic deformation is localized to within
 176 the shear zone and that the variation of that deformation along x occurs over a distance
 177 scale $d \gg h$. Consequently, scaling consideration of stress equilibrium within the shear
 178 zone implies that the shear stress τ satisfies $\partial\tau/\partial y = 0$: τ is uniform within $|y| < h/2$
 179 for a given x . We furthermore presume that the shear zone responds to deformation in
 180 linear viscous fashion, such that $\tau = \eta_f \dot{\gamma}$ where $\dot{\gamma}$ is twice the shear strain rate and η_f
 181 is the shear zone's viscosity. Because τ is uniform in y , $\dot{\gamma}$ is uniform along y as well. Ow-

182 ing to the condition that $d \gg h$, $\dot{\gamma} = \partial v_x / \partial y$ or $\partial v_z / \partial y$ for the in- and anti-plane strain
 183 cases, respectively, where v_x and v_z are the rates of displacement along the subscripted
 184 coordinates. Therefore, the displacement rate profile is as in Figure 1b and we may ex-
 185 press the uniform strain rate in y as $\dot{\gamma}(x, t) = V(x, t)/h$ where $V(x, t)$ is rate of rela-
 186 tive displacement of the top end of the shear zone with respect to the bottom in the x
 187 or z direction: i.e., for in-plane deformation, $V(x, t) = v_x(x, y = +h/2, t) - v_x(x, y =$
 188 $-h/2, t)$. The shear stress in the layer is then given by

$$189 \quad \tau(x, t) = \eta_f \frac{V(x, t)}{h} \quad (1)$$

190 We presume the material outside the layer responds in a linear elastic fashion, with
 191 shear modulus μ and Poisson ratio ν , to the internal inelastic deformation of the shear
 192 zone. The shear traction along the elastic bodies' boundaries at $y = \pm h/2$ is identically
 193 τ , owed to the continuity of traction across the boundaries. We denote the relative dis-
 194 placement of the shear zone $\delta(x, t)$, such that $V = \partial \delta / \partial t$, and for the in-plane case $\delta(x, t) =$
 195 $u_x(x, y = +h/2, t) - u_x(x, y = -h/2, t)$, where u_x is the displacement in the x direc-
 196 tion. Given that we are concerned with variations of deformation of the shear zone along
 197 x at scales $d \gg h$, we may effectively collapse the shear zone onto a fault plane along
 198 $y = 0$ and no longer give the layer explicit consideration. Due to the quasi-static, elas-
 199 tic deformation of the material external to the shear zone, the distribution of τ along
 200 the fault surface (i.e., the surface formerly demarcated along $y = \pm h/2$, and now along
 201 $y = 0^\pm$) must also satisfy

$$202 \quad \tau(x, t) = \frac{\mu'}{\pi} \int_{-\infty}^{\infty} \frac{\partial \delta(s, t) / \partial s}{s - x} ds + \tau_b(x, t) \quad (2)$$

203 where $\mu' = \mu/[2(1 - \nu)]$ and $\mu' = \mu/2$ for the in-plane and anti-plane cases, respec-
 204 tively. The last term on the right hand side is the shear tractions resolved on the fault
 205 plane due to external forcing while the first term is the change in shear tractions owed
 206 to a distribution of relative displacement, or slip, along the fault.

207

208 To draw useful comparisons later, we briefly consider here another configuration,
 209 one in which an elastic layer of thickness $b \gg h$ lies above the shear zone, and an elas-
 210 tic half-space lies underneath. In this case, when deformation along x occurs over dis-
 211 tances much longer than b , τ is instead given by [Viesca, 2016, supplementary materi-

212 als]

$$\tau(x, t) = E'b \frac{\partial^2 \delta(x, t)}{\partial x^2} + \tau_b(x, t) \quad (3)$$

214 where $E' = 2\mu/(1 - \nu)$ and $E' = \mu$ for the in-plane and anti-plane cases.

215

216 Combining (1) with (2) or (3) results in an equation governing the spatio-temporal
 217 evolution of slip δ . In the section that follows we first non-dimensionalize this equation
 218 and subsequently highlight the diffusive nature of fault slip evolution.

219 3 Problem non-dimensionalization

Positing a characteristic slip rate V_c , we may in turn define characteristic values
 of shear stress $\tau_c = \eta_f V_c/h$, time $t_c = h/V_c$, along-fault distance $x_c = \mu'h/\tau_c$ or $x_c =$
 $\sqrt{E'b h / \tau_c}$, and slip $\delta_c = h$. We update our notation going forward to reflect the fol-
 lowing nondimensionalization:

$$V/V_c \Rightarrow V, \tau_b/\tau_c \Rightarrow \tau_b, t/t_c \Rightarrow t, x/x_c \Rightarrow x, \text{ and } \delta/\delta_c \Rightarrow \delta$$

220 Doing so, the combination of (1) with (2) leads to

$$\frac{\partial \delta}{\partial t} = \mathcal{H} \left(\frac{\partial \delta}{\partial x} \right) + \tau_b(x, t) \quad (4)$$

222 where we identify the operator $\mathcal{H}(f) = (1/\pi) \int_{-\infty}^{\infty} f(s)/(s-x)ds$ on a spatial function
 223 $f(x)$ as the Hilbert transform. Useful properties of the Hilbert transform are that $\mathcal{H}[\mathcal{H}(f)] =$
 224 $-f$ and that it commutes with derivatives in time and space: e.g., $d[\mathcal{H}(f)]/dx = \mathcal{H}[df/dx]$.

225

226 For comparison, if we similarly combine and and non-dimensionalize (1) with (3),

$$\frac{\partial \delta}{\partial t} = \frac{\partial}{\partial x} \left(\frac{\partial \delta}{\partial x} \right) + \tau_b(x, t) \quad (5)$$

228 we immediately recognize that slip in this case satisfies the diffusion equation, with an
 229 external forcing term τ_b . While (5) is a classical problem with known solution, the dy-
 230 namics of (4), in contrast, has remained without comparable study despite being the sim-
 231 plest formulation of a rate-strengthening fault within an elastic continuum and despite
 232 also being among the simplest non-local, diffusion-type equations. However, in the sec-
 233 tions to follow we highlight that the linearity of problem (4), which we refer to as the
 234 Hilbert diffusion equation, makes it as amenable to solution as the classical diffusion equa-
 235 tion, though with several signature features.

236 **4 Solution via Green's function**

237 We begin by looking for the fundamental solution, also known as the Green's func-
 238 tion, to the problem in which the external forcing takes the form of an impulse at po-
 239 sition x' and time t' , i.e., the function $G(x, t; x', t')$ satisfying

240
$$\frac{\partial G}{\partial t} = \mathcal{H}\left(\frac{\partial G}{\partial x}\right) + \delta_D(x - x')\delta_D(t - t') \quad (6)$$

241 where we denote the Dirac delta function as $\delta_D(x)$. The impulse, represented by the last
 242 term in (6), corresponds to a line load of unit magnitude momentarily applied to the fault.

243

244 Following standard techniques (outlined in Appendix A), the Green's function for
 245 the Hilbert diffusion equation is, for $t > t'$

246
$$G(x, t; x', t') = \frac{1}{\pi(t - t')} \frac{1}{1 + \left(\frac{x - x'}{t - t'}\right)^2} \quad (7)$$

247 The Green's function exhibits self-similar behavior, in which distances x stretch with time
 248 t . While not explicitly considered as such, the Green's function solution was effectively
 249 also derived by *Ida* [1974] and *Ando et al.* [2012]. To contrast, we recall that the Green's
 250 function solution for classical diffusion is

251
$$G(x, t; x', t') = \frac{1}{\sqrt{4\pi(t - t')}} \exp\left[-\frac{(x - x')^2}{4(t - t')}\right] \quad (8)$$

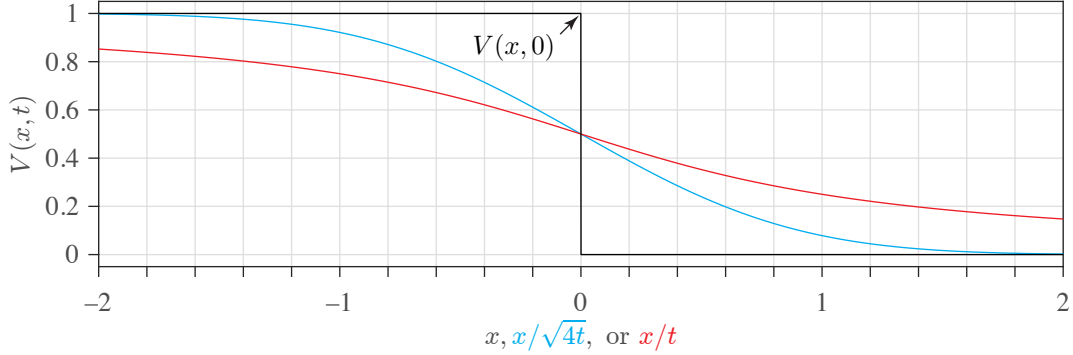
252 in which the power-law decay of the the Lorentzian $1/[\pi(1 + s^2)]$ gives way to the ex-
 253 ponential decay of a Gaussian and now distance x stretches with \sqrt{t} . This latter change
 254 could be anticipated from scaling of the equations (4) and (5), excluding the source term,
 255 in which we find that $[D]/[T] \sim [D]/[L]$ in (4) and $[D]/[T] \sim [D]/[L^2]$ in (5), where the
 256 scalings of slip, time, or length are denoted by $[D]$, $[T]$, and $[L]$, respectively.

257

258 Solutions to the problem of an arbitrary external forcing $\tau_b(x, t)$ are given by the
 259 convolution [e.g., *Carrier and Pearson*, 1976]

260
$$\delta(x, t) = \int_{-\infty}^{\infty} \int_{-\infty}^t G(x, t; x', t') \tau_b(x', t') dt' dx' \quad (9)$$

261 In the following section, we demonstrate the application of the Green's function solu-
 262 tion to solve two elementary problems: a sudden and semi-infinite or localized step in
 263 stress on the fault.



265 **Figure 2.** Similarity solutions (red and cyan) for slip rate V for a linear viscous fault having
 266 undergone an initial step in stress on $x < 0$, a problem equivalent to having the initial slip rate
 267 distribution shown in black. The cyan curve corresponds to the well-known error-function solu-
 268 tion (13) satisfying the classical diffusion equation and exhibits characteristic exponential decay.
 269 In contrast, the red curve, illustrating the solution (12) satisfying the Hilbert diffusion equation,
 270 exhibits power-law decay with a distinct similarity variable, x/t .

264 4.1 Example: Sudden step in stress

271 As a simple example we consider the problem in which a sudden step in stress of
 272 unit magnitude is applied at $t = 0$ and along $x < 0$, or

$$273 \tau_b(x, t) = H(-x)H(t) \quad (10)$$

274 A solution is readily found by recognizing that $\partial^2\delta/(\partial x\partial t)$ also satisfies the Hilbert dif-
 275 fusion equation except the forcing now corresponds to $\partial^2\tau_b/(\partial x\partial t) = -\delta_D(x)\delta_D(t)$, which
 276 is to within a sign of the Green's function problem with $x' = 0$ and $t' = 0$. Substi-
 277 tuting for the slip rate $V = \partial\delta/\partial t$, the solution to this second problem is given by the
 278 Green's function, i.e. for $t > 0$

$$279 \frac{\partial V}{\partial x} = -\frac{1}{\pi t} \frac{1}{1 + (x/t)^2} \quad (11)$$

280 and upon integration from $-\infty$ to x , with the condition that $V(-\infty, t > 0) = 1$ (i.e.,
 281 the unit slip rate corresponding to the unit step in stress) we find that

$$282 V(x, t) = \frac{1}{2} - \frac{1}{\pi} \arctan(x/t) = \frac{\operatorname{arccot}(x/t)}{\pi} \quad (12)$$

283 Problem (10) can be equivalently posed as the initial value problem $V(x, 0) = 1$ for $x <$
 284 0 and 0 otherwise. For comparison, the corresponding solution for the classical diffusion

285 equation is

$$286 \quad V(x, t) = \frac{1}{2} - \frac{1}{2} \operatorname{erf}(x/\sqrt{4t}) = \frac{\operatorname{erfc}(x/\sqrt{4t})}{2} \quad (13)$$

287 We illustrate these similarity solutions, as well as their initial condition, in Figure 2.

288

289 A solution to a similar problem, in which $\tau_b(x, t) = H(-x)\delta_D(t)$, was also solved
 290 by *Ida* [1974], using a complex variable approach. We can immediately see that, in the
 291 solution to this problem, slip takes the place of slip rate in (12), and that the problem
 292 can also be seen as the gradual smoothing of an initial dislocation of slip about $x = 0$,
 293 suddenly placed at $t = 0$. The solution procedure of *Ida* [1974] identified complex po-
 294 tential solutions to specific problems of (4), though appeared to overlook the self-similar
 295 nature of the solutions, the general Green's function solution procedure, and the diffu-
 296 sion connection.

297

298 A simple extension of the problem is the localized step in stress, given by

$$299 \quad \tau_b(x, t) = B(x)H(t) \quad (14)$$

300 where the boxcar function $B(x) = 1$ on $|x| < 1$ and 0 otherwise. The corresponding
 301 solution can be found using superposition of the pair of solutions to the problem (10),
 302 shifted to $x = \pm 1$

$$303 \quad V(x, t) = \frac{\arctan[(x+1)/t] - \arctan[(x-1)/t]}{\pi} \quad (15)$$

304 Figure 3a shows the solution at intervals in time.

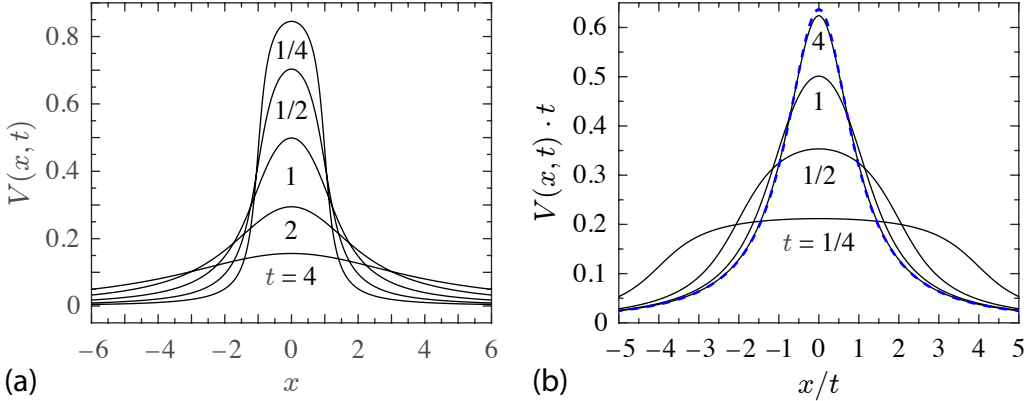
308 5 Self-similar asymptotics

309 Solutions to initial value problems exhibit self-similar behavior at long time: i.e.,
 310 an asymptotic expansion of solutions may be written in the limit $t \rightarrow \infty$ (Appendix
 311 B),

$$312 \quad V(x, t) = \sum_{n=1}^{\infty} \frac{1}{t^n} \operatorname{Re}[c_n f_n(\eta)] \quad \text{with } \eta = x/t \quad (16)$$

313 where the complex constants $c_n = a_n - ib_n$ and f_n are the complex functions

$$314 \quad f_n(\eta) = \frac{i}{\pi(\eta + i)^n} \quad (17)$$



305 **Figure 3.** (a) Solutions for slip rate at intervals of time t following an initial step in stress at
 306 $t = 0$ with a boxcar spatial distribution about $x = 0$. (b) Rescaling of the solutions in (a) to
 307 highlight the approach to the leading-order self-similar asymptotic solution (blue-dashed).

315 the real and imaginary parts of which are listed in Table 1 for the first several n . For
 316 initial conditions that vanish sufficiently fast outside of a finite region, the constants a_n
 317 and b_n are determined by the $(n-1)$ th moment of the initial distributions of V and $\mathcal{H}(V)$
 318 (Appendix C)

$$319 \quad a_n = \int_{-\infty}^{\infty} x^{n-1} V(x, 0) dx \quad (18)$$

$$320 \quad b_n = \int_{-\infty}^{\infty} x^{n-1} \mathcal{H}[V(x, 0)] dx \quad (19)$$

322 For sufficiently localized steps in stress, such as the first example in the following sub-
 323 section, the asymptotic expansion reduces to the series

$$324 \quad V(x, t) = a_1 \frac{g_1(\eta)}{t} + a_2 \frac{g_2(\eta)}{t^2} + O(t^{-3}) \quad (20)$$

325 where $g_n(\eta)$ are the real parts of $f_n(\eta)$. However, due to the long-range nature of elas-
 326 tic interactions in the crust, physical processes of interest will not typically have such
 327 a spatially compact loading. In the sub-sections to follow we will also consider two ex-
 328 amples in which the external forcing exhibits a slow decay in space. The first such ex-
 329 ample is a non-local step in stress whose solution follows simply from the localized load-
 330 ing problem considered. The last example examines an increase in fault slip rate induced
 331 by a specific physical process: the sudden slip of a small, secondary fault near a larger,
 332 rate-strengthening fault. This last example highlights additional considerations neces-
 333 sary to arrive to the appropriate asymptotic expansion.

334 **5.1 Example: Asymptotic behavior of a sudden step in stress**

Here we look for the asymptotic expansion for the problem (14), which corresponds to the initial value problem

$$V(x, 0) = B(x)$$

335 where $B(x)$ is the boxcar function introduced previously. For this case, the $(n - 1)$ th
336 moments of the initial distribution are

337
$$a_n = \int_{-1}^1 x^{n-1} dx = \begin{cases} 2/n & n \text{ odd} \\ 0 & n \text{ even} \end{cases} \quad (21)$$

338 To calculate the $(n - 1)$ th moments of $\mathcal{H}[V(x, 0)]$, we first find $\mathcal{H}[B(x)]$. To do so, we
339 use the commutative property of the Hilbert transform

340
$$\frac{d}{dx} (\mathcal{H}[B(x)]) = \mathcal{H}[B'(x)] = \mathcal{H}[\delta_D(x + 1) - \delta_D(x - 1)] = \frac{1}{\pi} \frac{1}{-1 - x} - \frac{1}{\pi} \frac{1}{1 - x} \quad (22)$$

341 and subsequently integrate to find that

342
$$\mathcal{H}[B(x)] = \frac{1}{\pi} \ln \left| \frac{1 - x}{1 + x} \right| \quad (23)$$

343 It then follows that the moments b_n do not exist as the integrals are divergent. Setting
344 $b_n = 0$, the asymptotic expansion is

345
$$V(x, t) = \frac{2}{\pi t} \frac{1}{1 + (x/t)^2} + \frac{2/3}{\pi t^3} \frac{3(x/t)^2 - 1}{[1 + (x/t)^2]^3} + \frac{2/5}{\pi t^5} \frac{5(x/t)^4 - 10(x/t)^2 + 1}{[1 + (x/t)^2]^5} + O(t^{-7}) \quad (24)$$

346 In Figure 3b we show that the general problem solution given by (15) converges to the
347 leading-order asymptotic term.

348 **Table 1.** Real and imaginary parts of $f_n(\eta)$ for $n = 1, \dots, 4$

n	$\text{Re}[\pi f_n(\eta)]$	$\text{Im}[\pi f_n(\eta)]$
1	$\frac{1}{1 + \eta^2}$	$\frac{\eta}{1 + \eta^2}$
2	$\frac{2\eta}{(1 + \eta^2)^2}$	$\frac{\eta^2 - 1}{(1 + \eta^2)^2}$
3	$\frac{3\eta^2 - 1}{(1 + \eta^2)^3}$	$\frac{\eta^3 - 3\eta}{(1 + \eta^2)^3}$
4	$\frac{4(\eta^3 - \eta)}{(1 + \eta^2)^4}$	$\frac{\eta^4 - 6\eta^2 + 1}{(1 + \eta^2)^4}$

349 **5.2 Example: A complementary problem**

350 To contrast with the preceding example, determining the asymptotic behavior of
 351 an initial value problem such as

352
$$V(x, 0) = -\frac{1}{\pi} \ln \left| \frac{1-x}{1+x} \right| \quad (25)$$

353 may at first appear to be problematic as the moments a_n do not exist. However, we re-
 354 call a result from the preceding example to note that

355
$$\mathcal{H}[V(x, 0)] = B(x) \quad (26)$$

356 Additionally, since $\mathcal{H}[V(x, t)]$ also satisfies the Hilbert diffusion equation (4), the asymp-
 357 totic behavior of $\mathcal{H}(V)$ is then precisely that of V in the preceding example

358
$$\mathcal{H}[V(x, t)] = \frac{2}{\pi t} \frac{1}{1 + (x/t)^2} + \frac{2/3}{\pi t^3} \frac{3(x/t)^2 - 1}{[1 + (x/t)^2]^3} + \frac{2/5}{\pi t^5} \frac{5(x/t)^4 - 10(x/t)^2 + 1}{[1 + (x/t)^2]^5} + O(t^{-7}) \quad (27)$$

359 Upon taking the Hilbert transform of both sides, we find the asymptotic decay of slip
 360 rate to follow

361
$$V(x, t) = \frac{2}{\pi t} \frac{x/t}{1 + (x/t)^2} + \frac{2/3}{\pi t^3} \frac{(x/t)^3 - 3(x/t)}{[1 + (x/t)^2]^3} + \frac{2/5}{\pi t^5} \frac{(x/t)^5 - 10(x/t)^3 + 5(x/t)}{[1 + (x/t)^2]^5} + O(t^{-7}) \quad (28)$$

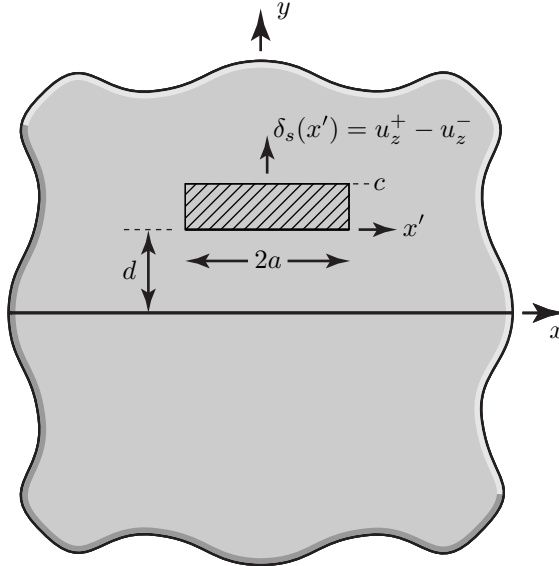
362 Alternatively, we may have directly calculated coefficients b_n (19)

364
$$b_n = \int_{-1}^1 x^{n-1} dx = \begin{cases} 2/n & n \text{ odd} \\ 0 & n \text{ even} \end{cases} \quad (29)$$

365 and with $a_n = 0$ retrieved the same expression (28) from (16).

370 **5.3 Example: Dislocation dipole near a principal fault**

371 We now consider the problem of sudden anti-plane slip within a region near a prin-
 372 cipal fault, as in Figure 4. Specifically, we imagine a secondary fault of length $2a$ lies par-
 373 allel to the principal fault and a distance d away. At $t = 0$ the secondary fault suddenly
 374 slips an amount c , which is represented by the sudden appearance of a pair of screw dis-
 375 locations with Burgers vectors of opposite signs a distance $2a$ apart, comprising a dis-
 376 location dipole. We are interested in determining the response of the principal fault to



366 **Figure 4.** Illustration of the model problem considered in Section 5.3, a relatively small
 367 secondary fault undergoes an amount c of relative anti-plane displacement δ_s at $t = 0$. The sec-
 368 ondary fault has a width $2a$ and is located a distance d away from the principal fault, which lies
 369 along the $x - z$ plane.

377 this perturbation. The off-fault dislocation dipole induce the stress change on the prin-
 378 cipal fault of the form

379

$$\tau_b(x, t) = \frac{c}{\pi} \left[\frac{x - a}{d^2 + (x - a)^2} - \frac{x + a}{d^2 + (x + a)^2} \right] H(t) \quad (30)$$

380 We may alternatively consider the posed problem as an initial value problem for the anti-
 381 plane slip rate of the principal fault

382

$$V(x, 0) = \frac{c}{\pi} \left[\frac{x - a}{d^2 + (x - a)^2} - \frac{x + a}{d^2 + (x + a)^2} \right] \quad (31)$$

383

384 One path to the full solution is to recognize that the function $h(x, t) = \mathcal{H}[V(x, t)]$
 385 also satisfies the Hilbert diffusion equation. We may now pose the problem as an initial
 386 value problem for $h(x, t)$ where

387

$$h(x, 0) = \mathcal{H}[V(x, 0)] = \frac{c}{\pi} \left[\frac{d}{d^2 + (x - a)^2} - \frac{d}{d^2 + (x + a)^2} \right] \quad (32)$$

388 Recognizing the form of the Green's function, the solution of the auxiliary problem is,
 389 by inspection,

$$390 \quad h(x, t) = \frac{c}{\pi(t+d)} \left[\frac{1}{1 + [(x-a)/(t+d)]^2} - \frac{1}{1 + [(x+a)/(t+d)]^2} \right] \quad (33)$$

391 The solution to the original problem then follows from the inversion for $V(x, t) = -\mathcal{H}[h(x, t)]$

$$392 \quad V(x, t) = \frac{c}{\pi(t+d)} \left[\frac{(x-a)/(t+d)}{1 + [(x-a)/(t+d)]^2} - \frac{(x+a)/(t+d)}{1 + [(x+a)/(t+d)]^2} \right] \quad (34)$$

393 where in the above we used the known transform $\mathcal{H}[x/(b^2 + x^2)] = b/(b^2 + x^2)$ for b a
 394 constant in space and the property that $\mathcal{H}\{\mathcal{H}[f(x)]\} = -f(x)$.

395

396 To find the asymptotic behavior, we look to determine the coefficients of the ex-
 397 pansion, a_n and b_n . However, this example is unlike the preceding ones owing to the power-
 398 law decay of both the initial slip rate and its Hilbert transform. Consequently, the mo-
 399 ment integral expressions for a_n and b_n as written in (18) and (19) are divergent for n
 400 sufficiently large. Nonetheless, we may proceed to determine the coefficients as follows.

401

402 First, given the problem symmetry, $V(x, t) = V(-x, t)$, we may anticipate that
 403 $a_n = 0$ when n is even and $b_n = 0$ when n is odd as we expect to keep only functions
 404 that are symmetric about $x = 0$ in the asymptotic expansion. Proceeding to determine
 405 the moments of the initial distribution and its Hilbert transform, leads to $a_1 = 0$ and
 406 $b_2 = 2ac$, the last of which we identify as the net moment of the dislocation dipole

407

$$m_o = 2ac$$

408 Examining the next-order moment a_3 , we find that the integral is divergent. This diver-
 409 gence is owed to the integrand approaching a finite value as $x \rightarrow \pm\infty$:

$$410 \quad \lim_{x \rightarrow \pm\infty} x^2 V(x, 0) = \frac{m_o}{\pi}$$

411 Subtracting this limit value from the integrand when calculating the moment, we find

$$412 \quad a_3 = \int_{-\infty}^{\infty} \left[x^2 V(x, 0) - \frac{m_o}{\pi} \right] dx = -m_o(2d)$$

413 The integrand of the moment b_4 likewise diverges due to the integrand having a non-zero
 414 limit in the far-field

$$415 \quad \lim_{x \rightarrow \pm\infty} x^3 \mathcal{H}[V(x, 0)] = -\frac{m_o(2d)}{\pi}$$

416 Proceeding similarly, we find that

$$417 \quad b_4 = \int_{-\infty}^{\infty} \left[x^3 \mathcal{H}[V(x, 0)] + \frac{m_o(2d)}{\pi} \right] dx = m_o(a^2 - 3d^2)$$

418 To determine the next-order coefficient a_5 , we note that as $x \rightarrow \infty$

$$419 \quad x^4 V(x, 0) \approx x^2 \frac{m_o}{\pi} + \frac{m_o(a^2 - 3d^2)}{\pi} + O(x^{-2})$$

420 the first two terms of which preclude the moment integral from being convergent. Sub-
421 tracting these terms from the moment integrand, we arrive to

$$422 \quad a_5 = \int_{-\infty}^{\infty} \left[x^4 V(x, 0) - x^2 \frac{m_o}{\pi} - \frac{m_o(a^2 - 3d^2)}{\pi} \right] dx = m_o[4d(d^2 - a^2)]$$

423

424 Thus, the four leading-order terms in the asymptotic expansion are

$$425 \quad V(x, t) = \frac{m_o}{\pi t^2} \frac{(x/t)^2 - 1}{[1 + (x/t)^2]^2} - \frac{m_o(2d)}{\pi t^3} \frac{3(x/t)^2 - 1}{[1 + (x/t)^2]^3} + \frac{m_o(a^2 - 3d^2)}{\pi t^4} \frac{(x/t)^4 - 6(x/t)^2 + 1}{[1 + (x/t)^2]^4}$$

$$426 \quad + \frac{m_o[4d(d^2 - a^2)]}{\pi t^5} \frac{5(x/t)^4 - 10(x/t)^2 + 1}{[1 + (x/t)^2]^5} + O(t^{-7}) \quad (35)$$

428 We emphasize that the leading term is independent of the distance d and dependent on
429 a and c only insofar as they determine the dipole moment m_o . Subsequent terms are found
430 following the procedure outlined above, i.e., given that $a_1 = 0$ and $b_2 = m_o$

$$431 \quad a_n = \int_{-\infty}^{\infty} \left[x^{n-1} V(x, 0) - \frac{1}{\pi} \sum_{k=1}^{(n-1)/2} x^{(n-1)-2k} b_{2k} \right] dx \quad \text{for } n = 3, 5, 7, \dots \quad (36)$$

$$432 \quad b_n = \int_{-\infty}^{\infty} \left[x^{n-1} \mathcal{H}[V(x, 0)] - \frac{1}{\pi} \sum_{k=1}^{(n-2)/2} x^{(n-2)-2k} a_{2k+1} \right] dx \quad \text{for } n = 4, 6, 8, \dots \quad (37)$$

434 6 Comparison with spring-block and finite-fault models

435 In the preceding section we found that the asymptotic response to a stress step is
436 a power-law decay in slip rate with time. In this section we highlight that such power-
437 law decay transitions to exponential decay in time if locked fault boundaries are encoun-
438 tered. This transition to a more rapidly decaying slip rate is owed to limitations of the
439 compliance of the coupled fault-host rock system. We begin by considering a simple sys-
440 tem with a limited compliance: a sliding block attached to a spring with fixed stiffness,
441 finding the exponential decay of slip rate following a step in stress. We subsequently ex-
442 amine a continuum system with limited compliance: a finite fault embedded within a full

space. We examine the response of such a fault to a step in stress and show that the decay of slip rate is expressible as the sum of orthogonal modes whose amplitudes have an exponential decay with time. We also highlight that the conditions for such asymptotic behavior are rather strict, requiring slip not penetrate beyond a particular position, and that non-exponential decay can be expected if fault boundaries are modeled as transitions in fault rheology.

6.1 Spring-block model

We consider a rigid block sliding on a rigid substrate. The block is attached to one end of a spring, with stiffness k , the other end of which is attached to a load point pulled at a constant rate V_p . The basal shear stress is denoted τ and τ_b is the shear stress applied to the top of the block. For quasi-static deformation,

$$\tau(t) = k[V_p t - \delta(t)] + \tau_b(t) \quad (38)$$

where $\delta(t)$ is both the basal slip and the displacement of the block. As before, we presume the basal interface is modeled as a thin viscous layer such that the interfacial shear strength is

$$\tau_s(t) = \eta \frac{V(t)}{h} \quad (39)$$

We consider the response to a sudden step in applied stress at $t = 0$

$$\tau_b(t) = \Delta\tau H(t) \quad (40)$$

With the initial condition $\delta(0) = 0$, the block's displacement relative to the load point is given by

$$\delta(t) - V_p t = (A - B)[1 - \exp(-t/t_c)] \quad (41)$$

where $t_c = \eta/(hk)$, $A = \Delta\tau/k$, and $B = V_p t_c$

6.2 Finite-fault model

We now consider the in-plane or anti-plane slip of a fault with a finite length $2L$. The dimensional shear stress on the fault plane is given by.

$$\tau(x, t) = \frac{\mu'}{\pi} \int_{-L}^L \frac{\partial \delta(s, t)/\partial s}{s - x} ds + \tau_b(x, t) \quad (42)$$

with the condition that there is no slip for $|x| > L$, including the endpoints: $\delta(\pm L, t) = 0$.

471

472 Nondimensionalizing as done previously to arrive to (4),

473
$$\tau(x, t) = \frac{1}{\pi} \int_{-\bar{L}}^{\bar{L}} \frac{\partial \delta(s, t)/\partial s}{s - x} ds + \tau_b(x, t) \quad (43)$$

474 where the dimensionless fault length is denoted $\bar{L} = L/x_c$. Requiring that $\tau = \tau_s$ within
475 the fault plane $|x| < \bar{L}$, the time rate of the above is

476
$$\frac{\partial V(x, t)}{\partial t} = \frac{1}{\pi} \int_{-\bar{L}}^{\bar{L}} \frac{\partial V(s, t)/\partial s}{s - x} ds + \frac{\partial \tau_b(x, t)}{\partial t} \quad (44)$$

477 with the condition that $V(\pm \bar{L}, t) = 0$.

478

479 We now look to determine how the finite fault responds to a step in stress $\tau_b(x, t) =$
480 $f(x)H(t)$. We may alternatively pose this problem as the initial value problem for the
481 slip rate as $V(x, 0) = f(x)$ where the slip rate for $t > 0$ satisfies

482
$$\frac{\partial V(x, t)}{\partial t} = \frac{1}{\pi} \int_{-\bar{L}}^{\bar{L}} \frac{\partial V(s, t)/\partial s}{s - x} ds \quad (45)$$

483 We begin by looking for solutions to (45) of the form

484
$$V(x, t) = \omega(x/\bar{L}) \exp(\lambda t/\bar{L}) \quad (46)$$

485 which, when substituted into (45) leads to the eigenvalue problem

486
$$\lambda \omega(x) = \frac{1}{\pi} \int_{-1}^1 \frac{d\omega(s)/ds}{s - x} ds \quad (47)$$

487 previously analyzed in the context of earthquake nucleation on linearly slip-weakening
488 faults [Dascalu *et al.*, 2000; Uenishi and Rice, 2003]. As discussed by those authors, so-
489 lutions to the eigen equation have the following properties: the eigenmodes ω_n are or-
490 thogonal and correspond to a set of discrete, unique eigenvalues $\lambda_n < 0$, which can be
491 arranged in decreasing order $0 > \lambda_1 > \lambda_2 \dots$. Consequently, the initial velocity distri-
492 bution can be decomposed into a sum of the eigenfunctions

493
$$V(x, 0) = \sum_{n=1}^{\infty} v_n \omega_n(x/\bar{L}) \quad (48)$$

494 where, owing to the orthogonality of ω_n , the coefficients of the expansion are given by

495
$$v_n = \frac{\int_{-1}^1 V(s\bar{L}, 0) \omega_n(s) ds}{\int_{-1}^1 \omega_n^2(s) ds} \quad (49)$$

496 and consequently, the solution to the initial value problem is

$$497 \quad V(x, t) = \sum_{n=1}^{\infty} v_n \omega_n(x/\bar{L}) \exp(\lambda_n t/\bar{L}) \quad (50)$$

498 The most slowly decaying symmetric and anti-symmetric modes can be accurately ap-
499 proximated, to within 1% besides an arbitrary scale factor, as

$$500 \quad \omega_1(x) \approx \sqrt{1 - x^2}(1 - x^2/3) \quad (51)$$

$$501 \quad \omega_2(x) \approx \sqrt{1 - x^2}[1 - (4x/5)^2]x \quad (52)$$

503 and have the eigenvalues $\lambda_1 = -1.157774\dots$ and $\lambda_2 = -2.754755\dots$. The eigenfunc-
504 tions and eigenvalues may be solved for numerically, as done by *Dascalu et al* [2000] us-
505 ing a Chebyshev polynomial expansion, *Uenishi and Rice* [2000] using a discrete dislo-
506 cation technique, or *Brantut and Viesca* [2015] using Gauss-Chebyshev-type quadrature
507 for a comparable problem. Doing so, (49) and (50) are then readily evaluated numer-
508 ically. The eigenfunction expansion can also be used to construct a Green's function so-
509 lution to the problem (43) or (44) with τ_b or $\partial\tau_b/\partial t$ being equal to $\delta(x - x')\delta(t - t')$,
510 which we defer to later work.

511

512 The finite-fault results here show what may be the fate of the self-similar spread-
513 ing of slip rate discussed in the preceding sections, which presumed that rigid bound-
514 aries are not yet encountered. Specifically, the self-similar behavior may be seen as in-
515 termediate: relevant when distributions of elevated slip rate extend over distances com-
516 parable to or greater than the initiating source, but still lie some distance away from locked
517 boundaries. If such boundaries are encountered, the self-similar behavior transitions to
518 one in which slip rate no longer spreads and instead decays in place exponentially with
519 time, akin to the behavior seen in spring-block models. In the following section we will
520 show that self-similar spreading implies a constant moment rate following a stress step.
521 We can immediately deduce from (50) that the moment rate, an integral of slip rate over
522 the fault, will ultimately exponentially decay back to zero from this constant value once
523 locked boundaries begin to influence slip rate within the fault interior. The rigidly locked
524 boundary condition may accurately represent the termination of a fault segment, in which
525 a fault discontinuity transitions to intact rock. However, a more accurate boundary con-
526 dition for mature faults, which may slow down the abrupt, exponential decay of slip rate,

527 may be a rheological transition accompanying increases in temperature down dip, or het-
 528 erogeneity in fault material properties along strike.

529 **7 Discussion**

530 **7.1 Relation with existing spring-block and continuum models for post-**
 531 **seismic slip**

532 Observations of surface displacements that appear to increase logarithmically with
 533 time have been used as evidence for postseismic deformation due to frictional afterslip
 534 or ductile deformation of faults, in part owed to the observation that such a logarithmic
 535 time dependence arises in models of stable fault slip. Early models have focused on the
 536 displacement response of spring-block systems to steps in stress, and a logarithmic in-
 537 crease of displacement has been shown to arise in models that include an explicit depen-
 538 dence of strength on the logarithm of the sliding rate, including slip rate- and state-dependent
 539 strength descriptions [e.g., Marone *et al.* 1991; Perfettini and Avouac, 2004; Montesi,
 540 2004; Helmstetter and Shaw, 2009]. In general, however, spring-block models in which
 541 the frictional strength linearizes about a finite or zero value of slip rate—including slip
 542 rate- and state-dependent friction—all exhibit a slip rate that, at sufficiently long time,
 543 relaxes back to a zero or finite value exponentially with time following a step in stress,
 544 under a negligible or finite value of the load-point velocity V_p . Nonetheless, a logarith-
 545 mic growth of displacement can arise from a spring-block model in some limiting cases
 546 when considering a frictional formulation that does not linearize about $V = 0$, specif-
 547 ically a strength relation $\tau_s(V) = \tau_o + c \ln(V)$. Revisiting the analysis of Section 6.1
 548 for the response of a spring-block system to a sudden step in stress and replacing the lin-
 549 ear viscous strength relation with this logarithmic slip-rate dependence, one finds that
 550 the asymptotic behavior is $V \sim 1/t$, and hence $\delta \sim \ln(t)$, provided that the load point
 551 velocity $V_p = 0$. For finite values of V_p , the slip rate approaches a $1/t$ decay only as an
 552 intermediate asymptote at sufficiently short times after the step, followed by a transi-
 553 tion to an exponential decay of slip rate to the finite value of V_p at long time.

554

555 That strength may depend on the logarithm of slip rate is consistent with exper-
 556 imental observations and the constitutive formulation for rate- and state-dependent fric-
 557 tion insofar as these both exhibit a logarithmic dependence under steady-sliding condi-

tions [Dieterich, 1978, 1979; Ruina, 1980, 1983]. Considering that the full rate- and state-dependence, with aging-law state evolution, does not qualitatively change the behavior following a step in stress applied to a spring-block system in comparison with a strictly logarithmic dependence on slip rate: a $1/t$ decay shortly after the step transitions to oscillatory exponential decay at long time [e.g., Rice and Ruina, 1983; Helmstetter and Shaw, 2009]. This has made the spring-block model a common representation of post-seismic fault slip when attempting to fit observed displacements with the functional form $\delta(t) = \delta_c \ln(1 + t/t_c)$, and the goodness of fit has furthermore been taken as evidence in support of a rate- and state-dependent description governing fault strength in the post-seismic period. Specifically, the spring-block model of Marone *et al.* [1991] is based on the strict logarithmic dependence and $V_p = 0$, while Perfettini and Avouac [2004] relax the latter assumption and Helmstetter and Shaw [2009] consider the full rate- and state-dependent formulation and show the limiting cases where a $1/t$ decay in slip rate may arise.

571

However, we find that a logarithmic dependence on time of both displacement on the fault—as well as that at a free surface—also emerges from a fault with a simple linear viscous strength. This emergence is owed to the interactions between points on the fault that accompany a continuum description, which is neglected in spring block models. The logarithmic dependence is readily seen for fault displacement given the asymptotic expansion for slip rate (16) following a step in stress on the fault, which at the leading order has $a_1 \neq 0$ and $b_1 = 0$, and provides the asymptotic form of fault slip upon integration

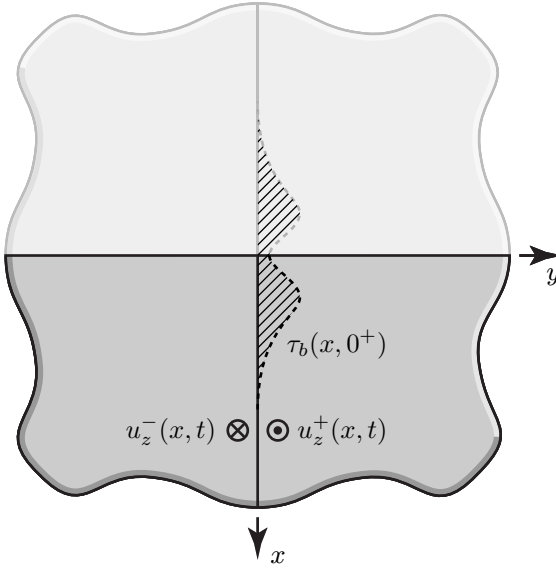
$$\delta(x, t) = \delta_0 + \frac{a_1}{\pi} \ln(x^2 + t^2) + O(t^{-1}) \quad (53)$$

where δ_0 is a constant.

582

588

How will the asymptotic decay of slip rate on the fault be reflected at displacement on the surface? We consider a simple model of a long, vertical fault that undergoes strike-slip (anti-plane) motion and intersects the free surface, lying along $x \geq 0$ (Figure 5). For simplicity, we imagine that the fault has undergone a sudden step in shear stress with some distribution along $x \geq 0$. The solution to this problem is found by method of im-



583 **Figure 5.** An anti-plane fault in the x - z plane intersects a free surface at $x = 0$. The solution
 584 to a sudden step in stress τ_b at $t = 0^+$ along the fault ($x > 0$) is found by method of images.
 585 The image problem is shown as a transparent continuation in the upper half plane, $x < 0$. The
 586 hatched area represents the net force exerted on the imaged fault per unit distance along strike,
 587 which determines the leading-order coefficient of the asymptotic expansion, a_1 .

594 ages [e.g., Segall, 2010], in which the original problem is reflected about $x = 0$ such that
 595 the fault now lies in a full space with a step in stress symmetric about $x = 0$. The so-
 596 lution for the half-space problem is the full-space solution for $x \geq 0$. Given the fault
 597 slip rate $V(x, t)$, the dimensionless out-of-plane displacement rate off the fault is

$$598 v_z(x, y, t) = \frac{1}{2\pi} \int_{-\infty}^{\infty} \frac{\partial V(s, t)}{\partial s} \arctan\left(\frac{s-x}{y}\right) ds \quad (54)$$

601 which follows from the superposition of the solution for the displacement field surrounding
 602 a screw dislocation in an infinite medium [e.g., Hirth and Lothe, 1982]. Given that
 603 the fault slip rate for this problem decays at long time as

$$602 V(x, t) = \frac{a_1}{\pi t} \frac{1}{1 + (x/t)^2} + \frac{a_3}{\pi t^3} \frac{3(x/t)^2 - 1}{[1 + (x/t)^2]^3} + O(t^{-5}) \quad (55)$$

603 the substitution of the spatial derivative of this expansion into (54) and the evaluation
 604 of the integral for positions at the surface ($x = 0$) reveals that the displacement rate
 605 there decays as

$$606 v_z(0, y, t) = \frac{a_1}{2\pi} \frac{1}{(y+t)} + O(t^{-3}) \quad (56)$$

and the long-time behavior of the surface displacement follows from the time integration of (56)

$$u_z(0, y, t) = u_0 + \frac{a_1}{2\pi} \ln(y + t) + O(t^{-2}) \quad (57)$$

where u_0 is a constant of integration. Here we see that the expected long-time evolution of the surface displacement is logarithmic with time. As we will come to see in the following section, the coefficient of the logarithm a_1 represents the net force exerted (per unit distance perpendicular to strike) on the fault by the sudden increase in shear stress.

We highlight how quickly the logarithmic time dependence is approached by using a simple initial stress step example: $\tau_b(x, t) = B(x)H(t)$ for $x > 0$. The full slip rate solution for the half-space follows from the example problem considered previously in Section 4 for the full space and is given by (15) with $x > 0$. Using this, we directly calculate the displacement history on one side of the fault $y = 0^+$ at the surface $x = 0$

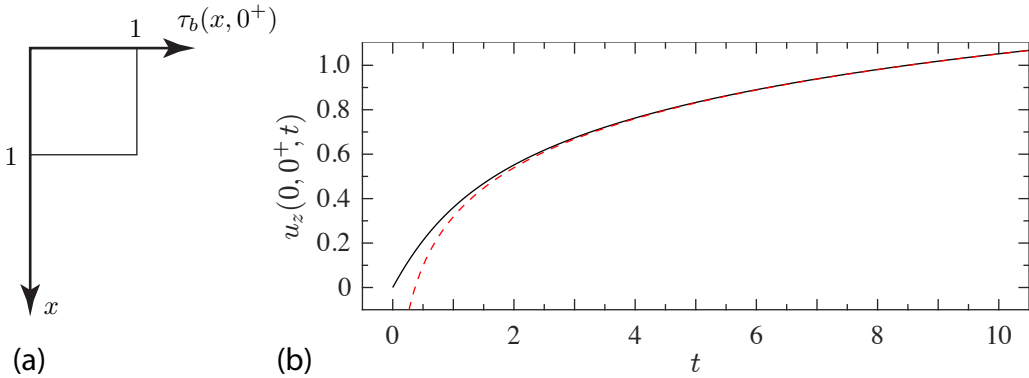
$$\begin{aligned} u_z(0, 0^+, t) &= \int_0^t v_z(0, 0^+, t') dt' \\ &= \frac{1}{\pi} t \arctan(1/t) + \frac{1}{2\pi} \ln(1 + t^2) \end{aligned} \quad (58)$$

The behavior of which as $t \rightarrow \infty$ is

$$u_z(0, 0^+, t) = \frac{1}{\pi} + \frac{1}{\pi} \ln(t) \quad (59)$$

which, apart from the constant of integration u_0 , we could have deduced directly from (57) given that $a_1 = 2$ for this example, and $y = 0^+$ for the point of interest here. In Figure 6 we overlay the asymptotic solution on the full displacement history for this example, and show the rapid convergence of the latter to the former.

To clearly outline the interplay between continuum deformation and fault rheology and to highlight its consistency with observations, we have thus far considered relatively simple model geometries; however, an extensive effort of using forward models of frictional faults embedded in a continuum to account for geodetic afterslip observations has accompanied both the increase in GPS data and computational resources needed to run many iterations of the forward models for parameter inversion. *Linker and Rice* [1997] sought to reproduce the observed postseismic deformation following the Loma Pri-



627 **Figure 6.** (a) Illustration of a boxcar step in stress with depth x on an anti-plane (strike-slip)
 628 fault, beginning at $t = 0^+$. (b) Evolution of the anti-plane displacement component u_z at the free
 629 surface ($x = 0$) to one side of the fault ($y = 0^+$), given by (58) (black), following the step in fault
 630 shear stress; the displacement quickly approaches the logarithmic asymptote (59) (red-dashed).

639 eta earthquake, considering several model fault geometries while comparing the response
 640 to a sudden step in stress of a linear viscoelastic fault rheology with a so-called hot-friction
 641 model, $\tau \sim \ln V$, intended to mimic the steady-state behavior of rate- and state-dependent
 642 friction. Both models provided comparable fits to the surficial displacements, with the
 643 conclusion that while deep relaxation process may be adequate, discriminating among
 644 different rheological models remains an issue. This continued to be reflected in subse-
 645 quent efforts, including that of *Hearn et al.* [2002], who considered geodetic observations
 646 of postseismic deformation in response to the 1999 Izmit earthquake. The authors per-
 647 formed a parameter inversion using a forward model to determine whether postseismic
 648 deformation in response to a co-seismic step in shear stress arises by viscoelastic relax-
 649 ation of the lower crust, poroelastic rebound, or via a fault slip on regions at depth whose
 650 strength obeys a linear viscous strength of the type examined here or the logarithmic
 651 hot-friction model also used in *Linker and Rice* [1997] and *Marone et al.* [1991]. While
 652 poroelastic rebound was quickly ruled out and the frictional afterslip models offered im-
 653 provements over the strictly viscoelastic model, the discrepancies between fault models
 654 with linear and logarithmic slip-rate dependence were marginal.

655

656 That different frictional models may have consistent asymptotic behavior is fur-
 657 ther supported when considering numerical studies of stable afterslip. *Hetland et al.* [2010]

examined numerical solutions for the post-seismic response to imposed co-seismic stress changes on vertical strike-slip (anti-plane) faults that obeyed a wide range of frictional constitutive relations, ranging from linear and power-law non-linear viscous to logarithmic hot friction and rate- and state-dependence. The authors focus on the latter two relations and the numerical results show that the long-time decay of slip rates at a fixed position follow the expected $1/t$ decay anticipated by our analytical treatment here, given that the models examined are expected to relax back to the finite, model-driving slip rate about which these non-linear constitutive relations can be linearized. Our expected $1/t$ decay, as well as a spatial spreading of elevated slip rates that is proportional to time, is also reflected in several other numerical studies of rate-strengthening faults [e.g., *Ariyoshi et al.*, 2007; *Perfettini and Ampuero*, 2008]

669

While the issue of determining the relative contributions of different mechanisms to postseismic deformation remains, cases in which afterslip appears to be the dominant mechanism [e.g., *Freed*, 2007] do appear to be well modeled as the accelerated creep of a fault with a rate- (and possibly state-) dependent friction [e.g., *Johnson et al.*, 2006; *Barbot et al.*, 2009]; however, such studies focus on a single fault strength description or rheology and comparatively little effort has been made to determine whether a particular rate-strengthening rheology is called for among several plausible ones [*Montési*, 2004]. That disparate, non-linear rheological relations may share a common asymptotic behavior indicates that such an effort to discriminate requires careful attention.

679

7.2 Moment-duration scalings of spontaneous slow slip events

Another potential observational constraint on fault strength follows from slow slip events on subduction faults that occur without the accompaniment of a large earthquake. These events were first observed geodetically [*Hirose et al.*, 1999; *Dragert et al.*, 2001] and subsequently found to be accompanied by seismic tremor [*Rogers and Dragert*, 2003; *Obara et al.*, 2004; *Obara and Hirose*, 2006]. Compiled estimates of moment release and duration of subduction zone slow slip events appear to show a linear relationship between these quantities [*Schwartz and Rokosky*, 2007; *Ide et al.*, 2007; *Aguiar et al.*, 2009; *Gao et al.*, 2012; *Liu*, 2014]. Slow slip events were shown to emerge spontaneously from fault models with slip rate- and state-dependent friction under marginal conditions for fric-

689 tional instability [Liu and Rice, 2005, 2007; Rubin, 2008]. Numerical models are capa-
 690 ble of producing a range of event sizes with a moment-duration relation that is arguably
 691 linear [Shibazaki *et al.*, 2012; Liu, 2014; Li and Liu, 2016; Romanet *et al.*, 2018]; how-
 692 ever, a mechanistic explanation for the emergence of such a scaling has been missing, mak-
 693 ing it difficult to assess the robustness of and the necessary conditions for the observed
 694 model scaling.

695

696 Here we highlight alternative conditions permitting the existence of slow slip and
 697 show that a linear moment-duration scaling arises naturally from the stable response of
 698 a rate-strengthening fault to a stress perturbation or sudden elevation of pore fluid pres-
 699 sure. For simplicity, we focus on the example of a fault undergoing in-plane or anti-plane
 700 rupture, in which slip varies only along one dimension; however, the same conclusion can
 701 be reached following a similar line of argument given comparable slip-rate self-similarity
 702 on a fault undergoing mixed-mode rupture, in which slip varies in two dimensions.

703

704 For a fault in which slip varies along one dimension, the moment per unit fault thick-
 705 ness in the out-of-plane direction is defined as

$$706 M(t) = \mu \int_{-\infty}^{\infty} \delta(x, t) dx \quad (60)$$

707 and the moment rate is, using dot notation to denote a derivative with respect to time,

$$708 \dot{M}(t) = \mu \int_{-\infty}^{\infty} V(x, t) dx \quad (61)$$

709 where in the two equations above we have momentarily returned to using dimensional
 710 variables. We now pass to non-dimensional variables as done to arrive to (4) and for the
 711 moment and moment rates using $M(t)/(\mu\delta_c x_c) \Rightarrow M(t)$ and $\dot{M}(t)/(\mu V_c x_c) \Rightarrow \dot{M}(t)$.
 712 We are interested in the asymptotic evolution of the fault moment release with time du-
 713 ration t following a step in stress. Substituting the asymptotic expression for fault slip
 714 rate following a step in stress (55), we find that the moment rate to leading order is con-
 715 stant, i.e.,

$$716 \dot{M}(t) = \frac{a_1}{\pi t} \int_{-\infty}^{\infty} \frac{1}{1 + (x/t)^2} dx = a_1 \quad (62)$$

717 The constant a_1 can be interpreted as the net increase of force on the fault, per unit out-
 718 of-plane fault thickness, owed to the distributed stress step: i.e., for a stress step in the

719 form $\tau_b(x, t) = \Delta\tau(x)H(t)$

$$720 \quad a_1 = \int_{-\infty}^{\infty} \Delta\tau(x)dx \quad (63)$$

721 This representation is seen by recognizing that the integral defining a_1

$$722 \quad a_1 = \int_{-\infty}^{\infty} V(x, 0)dx \quad (64)$$

723 directly follows, given the relation $\tau = V$, from the more general statement of conser-
724 vation for $t > 0$

$$725 \quad a_1 = \int_{-\infty}^{\infty} \tau(x, t)dx \quad (65)$$

726 which is itself deduced by demonstrating that, for $t > 0$

$$727 \quad \frac{d}{dt} \int_{-\infty}^{\infty} \tau(x, t)dx = 0 \quad (66)$$

728 by substituting the expression (4) for the fault shear stress τ , recognizing that $\partial[\mathcal{H}(\partial\delta/\partial x)]/\partial t =$
729 $\partial\mathcal{H}(V)/\partial x$, and using the condition that $\mathcal{H}(V)$ vanishes at $x = \pm\infty$. This implies that,
730 for $t > 0$

$$731 \quad a_1 = \int_{-\infty}^{\infty} \tau_b(x, t)dx \quad (67)$$

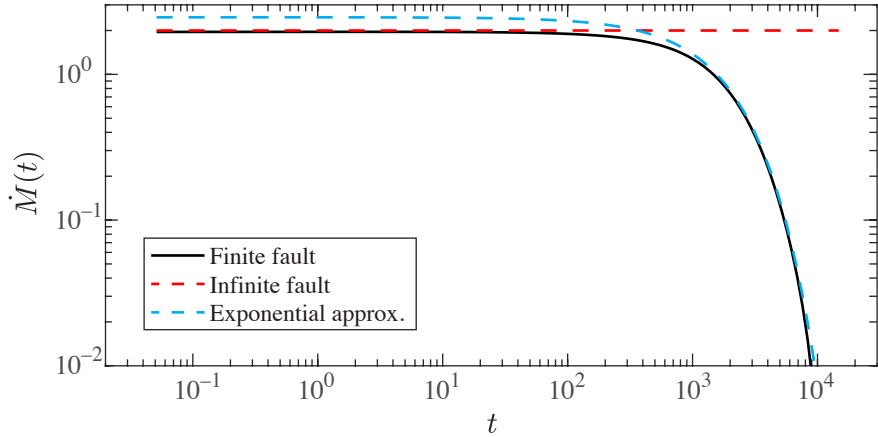
732 from which (63) follows.

733

734 The above conservation condition on the net shear force exerted on the fault by
735 the shear stress change, which implied a constant moment rate, is independent of the fault
736 elastic configuration and mode of slip. In other words, while we considered the partic-
737 ular case of in- or anti-plane slip between elastic half-spaces, a constant moment rate would
738 also be expected for any configuration—including mixed-mode slip between elastic half-
739 spaces, or in proximity to a free surface—in which the fault strength is proportional to
740 the sliding rate. By corollary, this also implies that a constant moment rate would ul-
741 timately be expected for non-linear, rate-dependent (and rate-strengthening) descrip-
742 tions of fault strength, which can be considered to approach an effective linear-viscous
743 response as the fault relaxes back to a steady sliding velocity.

744

745 The duration of the constant moment rate cannot be indefinite. As noted in Sec-
746 tion 6.2, locked boundaries will lead to exponential decay of the slip and moment rates.
747 In Figure 7 we show this transition in the moment rate of a fault that experiences a sud-
748 den step in stress at $t = 0$ with a boxcar distribution of unit magnitude, as in Sections



758 **Figure 7.** Plot of moment rate with time following a boxcar step in stress of unit magnitude
 759 and within a unit distance about the origin of a finite fault whose half-length $L = 1000$. The
 760 initial moment rate is constant, as expected for an unbounded fault (red-dashed), followed by the
 761 exponential decay (cyan-dashed) expected from the finite-fault analysis.

749 4.1 and 5.1, except here the fault is of finite length $2L = 2000$, a length much larger
 750 than the initial step in stress occurring over distances $|x| < 1$. As expected, at early times
 751 the finite fault boundaries are not apparent and the initial moment rate is constant and
 752 corresponds to the integrated step in stress, or equivalently the coefficient a_1 , implying
 753 $\dot{M} = 2$. At late times, the fault boundaries are manifest and the rapid, exponential de-
 754 cay of the moment rate follows. The exponential decay is captured by the dominant mode
 755 of the expansion (50), whose spatial distribution is approximated by (51), the exponen-
 756 tial decay rate is $\lambda_1 = -1.157774\dots$, and the prefactor $v_1 \approx 0.0017$ is calculated using
 757 the initial condition via (49).

762

763

764 While we have thus far shown that the moment release following a step in stress
 765 is initially linear in time, we have not yet identified potential mechanisms for such a step
 766 that would initiate a slow slip event. While there may be potential causes for a fault to
 767 experience an increase in shear stress, we briefly outline here conditions by which an in-
 768 crease in pore fluid pressure could lead to a slow slip event with a linear moment-duration
 769 relationship. Specifically, we assume fault strength is frictional in nature and rate-strengthening
 770 with the simple form $f(V) = f_o + cV$, where here and in what follows we continue the

dimensionless representation for brevity. The frictional nature of the strength implies that the shear strength can be written as $\tau_s = \bar{\sigma}f$ where $\bar{\sigma}$ is the effective normal stress $\bar{\sigma} = \sigma - p$, the difference between the total fault-normal stress σ and the fault pore fluid pressure p . We consider a sudden increase in pore fluid pressure beyond an initial value p_o of the form $p(x, t) = p_o + \Delta p(x)H(t)$, where we neglect here details of the fluid pressure evolution, but simply assume the rise time is short and the distribution is compact in space. The requirement that $\tau_s = \tau$ when and where sliding occurs can then be rearranged to have a form comparable to that of a shear stress step on a fault with linear viscous strength

$$\frac{\partial V}{\partial t} = \mathcal{H} \left(\frac{\partial V}{\partial x} \right) + \Delta\tau(x)\delta_D(t) \quad (68)$$

for which we have just shown that the integral of $\Delta\tau(x)$ is a conserved quantity that determines the constant moment rate at long times. For the problem of a pore pressure step considered here, we may identify $\Delta\tau(x)$ with $f_o\Delta p(x)$. Therefore, such a sudden increase in pore pressure would also give rise to the transient slip phenomena discussed in the preceding sections for local steps in shear stress.

8 Conclusion

We examined the evolution of slip and slip rate between elastic half-spaces that is accommodated as the shear of an adjoining thin, viscous layer. The model provides an elementary description of stable, yet transient, fault slip and also provides a basis with which to examine non-linear, rate-dependent descriptions of fault strength. The problem reduces to an integro-differential equation for slip or slip rate that has an analogy with the classical diffusion equation, in which slip or slip rate takes the place of temperature and sources of fault shear stress take the place of sources of heat. The new problem governing fault slip evolution, which we refer to as Hilbert diffusion, has several distinctive features. In classical diffusion, the interaction among points in space is mediated by second-order spatial derivatives and is short-ranged, having a characteristic exponential decay; for viscous slip between elastic half-spaces, the interaction is now long-ranged with a characteristic power-law decay. Furthermore, while classical diffusion exhibits diffusive spreading proportional to the square-root of time, the Hilbert diffusion problem exhibits spreading proportionally to time, such that distinct features, like local maxima of slip or stress rates, may have an apparent propagation velocity.

The response of faults to sudden changes in shear stress yields a slip rate that decays as $1/t$ such that near-fault displacements grow logarithmically with time. Examining a simple fault system, this logarithmic growth of displacement extends to that observed at the surface. This suggests that the observed logarithmic time-dependence of geodetic, post-seismic displacement measurements may be a symptom of post-seismic slip on rate-strengthening faults. This is a relaxation from previous, post-seismic slip models of such deformation, which hinged on a specific non-linear constitutive form of fault rate strengthening (i.e., logarithmic dependence on slip rate) and the single-degree-of-freedom nature of the elastic deformation. Instead, we suggest that, when considering the continuum deformation of an elastic medium in response to fault slip, it may not be possible to discriminate on the particular form of the non-linearity of the frictional strength description on the basis of long-term surface measurements. This suggestion is provided that fault boundaries or rheological transitions do not play a determining role in limiting the spatial penetration of post-seismic slip. Furthermore, we highlight that, in the absence of locked boundaries, a linear rate-strengthening rheology necessarily implies that the scaling of moment with duration is linear in time. This scaling is consistent with inferences of such a relationship for slow slip transients and suggests that slow slip may be a manifestation of a rate-strengthening fault response to transient increases in fault shear stress or pore fluid pressure, the latter provided that the rate-dependence of strength is frictional in nature.

823 A: Solution for Green's function

824 Here we provide details of the solution for the Green's function of the Hilbert diffusion equation. We denote the combined Fourier and Laplace transform of the slip distribution in space and time, respectively, as

$$827 D(k, s) = \int_{-\infty}^{\infty} e^{-2\pi i k x} \int_{-\infty}^{\infty} e^{-st} \delta(x, t) dt dx \quad (\text{A.1})$$

828 Taking the combined transform of

$$829 \frac{\partial \delta}{\partial t} = \mathcal{H} \left(\frac{\partial \delta}{\partial x} \right) + \delta_D(x - x') \delta_D(t - t') \quad (\text{A.2})$$

830 and using the properties of each transform with respect to derivatives, convolutions, and
831 the Dirac delta leads to

$$832 sD(s, k) = -2\pi|k|D(k, s) + e^{-2\pi i k x'} e^{-st'} \quad (\text{A.3})$$

833 or, after rearranging,

834

$$D(s, k) = \frac{e^{-2\pi i k x'} e^{-st'}}{s + 2\pi |k|} \quad (\text{A.4})$$

835

836 The inverse Laplace transform of $A(k) \exp(-st')/[s+B(k)]$ is $A(k) \exp[-B(k)(t-t')]$
 837 where $A(k) = e^{-2\pi i k x'}$ and $B(k) = 2\pi |k|$ and $H(x)$ is the Heaviside step
 838 function. The Green's function (7) then follows from the inverse Fourier transform. Ando
 839 et al. [2012], following Ida [1974], effectively arrived to this solution previously when con-
 840 sidering a problem equivalent to (A.2) with $x' = 0$ and $t' = 0$, though did not explic-
 841 itly consider their solutions in terms of a fundamental solution as done here.

842 **B: Similarity solutions for slip rate**

843 We look for similarity solutions for slip rate satisfying the Hilbert diffusion equa-
 844 tion

845

$$\frac{\partial V}{\partial t} = \mathcal{H} \left(\frac{\partial V}{\partial x} \right) \quad (\text{B.1})$$

846 of the form $V(x, t) = U[\eta(x, t), \tau(t)]$ where $\eta = x/t$, $\tau = \ln t$ [e.g., Barenblatt, 1996].
 847 Substituting our ansatz into (B.1),

848

$$\frac{\partial U}{\partial \tau} - \eta \frac{\partial U}{\partial \eta} = \mathcal{H} \left(\frac{\partial U}{\partial \eta} \right) \quad (\text{B.2})$$

849 We now look for solutions decomposed as

850

$$U(\eta, \tau) = f(\eta) \exp(\lambda \tau) \quad (\text{B.3})$$

851 which leads to the eigenvalue problem for eigenmodes λ and eigenfunctions $f(\eta)$

852

$$\lambda f - \eta f' = \mathcal{H}(f') \quad (\text{B.4})$$

853 If f is an analytic function, we may write its real and imaginary parts as $f(\eta) = g(\eta) +$
 854 $ih(\eta)$, where $g = \mathcal{H}(h)$ (Appendix D). Consequently, $\mathcal{H}(f) = if$, and (B.4) reduces
 855 to

856

$$\lambda f = (i + \eta)f' \quad (\text{B.5})$$

857 which has the solution

858

$$f(\eta) = A(i + \eta)^\lambda \quad (\text{B.6})$$

859 where A is a complex constant. Imposing boundary conditions that f vanishes as $\eta \rightarrow$
 860 ∞ , restricts $\lambda \leq 0$ and further requiring that f have similar asymptotic behavior as $\eta \rightarrow$

861 $\pm\infty$ implies that λ has an integer value: i.e., $\lambda = -n$ where $n = 1, 2, 3\dots$ and we de-
862 note the set of eigenfunctions as

$$863 \quad f_n(\eta) = \frac{i}{\pi(i + \eta)^n} \quad (\text{B.7})$$

864 where the choice of prefactor $A = i/\pi$ is made for $\text{Re}[f_1(\eta) \exp(-\tau)]$ to correspond with
865 the Green's function.

866 C: Long-time asymptotic expansion of initial value problem

867 We are interested in determining the long-time asymptotic behavior of solutions
868 for a sudden step in stress of the form

$$869 \quad \tau_b(x, t) = T(x)H(t) \quad (\text{C.1})$$

870 which can also be considered as an initial value problem

$$871 \quad V(x, 0) = T(x) \quad (\text{C.2})$$

872 Specifically, we look to determine the complex coefficients $c_n = a_n - ib_n$ for an asymp-
873 totic expansion of slip rate of the form

$$874 \quad V(x, t) = \sum_{n=1}^{\infty} \frac{1}{t^n} \text{Re}[c_n f_n(\eta)] \quad (\text{C.3})$$

875 for an initial value problem in slip rate.

876

877 We begin with the Green's function solution to the problem

$$878 \quad V(x, t) = \frac{1}{\pi t} \int_{-\infty}^{\infty} V(x', 0) \frac{1}{1 + [(x - x')/t]^2} dx' \quad (\text{C.4})$$

879 Recalling the Taylor expansion about $\epsilon = 0$

$$880 \quad \frac{1}{1 + \epsilon} = 1 - \epsilon + \epsilon^2 - \epsilon^3 + \dots = \sum_{k=0}^{\infty} (-1)^k \epsilon^k \quad (\text{C.5})$$

881 we may expand the Green's function about large time as

$$882 \quad V(x, t) = \frac{1}{\pi t} \int_{-\infty}^{\infty} V(x', 0) \left[\sum_{k=0}^{\infty} (-1)^k \left(\frac{x - x'}{t} \right)^{2k} \right] dx' \quad (\text{C.6})$$

883 Using the binomial expansion

$$884 \quad (a + b)^j = \sum_{i=1}^j \binom{j}{i} a^{j-i} b^i \quad (\text{C.7})$$

885 we may rewrite (C.6) as

$$886 \quad V(x, t) = \frac{1}{\pi t} \int_{-\infty}^{\infty} V(x', 0) \left[\sum_{k=0}^{\infty} \sum_{i=1}^{2k} \frac{(-1)^{k+i}}{t^{2k}} \binom{2k}{i} x^{2k-i} x'^i \right] dx' \quad (\text{C.8})$$

887 and swapping the order of summation

$$888 \quad V(x, t) = \frac{1}{\pi t} \int_{-\infty}^{\infty} V(x', 0) \left[\sum_{i=0}^{\infty} \sum_{k=0}^{\infty} \frac{(-1)^{k+i}}{t^{2k}} \binom{2k}{i} x^{2k-i} x'^i \right] dx' \quad (\text{C.9})$$

889 where the binomial coefficient is understood here to be zero if $2k < i$. We may then

890 rearrange

$$891 \quad V(x, t) = \sum_{i=0}^{\infty} \frac{1}{t^{i+1}} \left[\int_{-\infty}^{\infty} V(x', 0) x'^i dx' \right] \left[\frac{1}{\pi} \sum_{k=0}^{\infty} (-1)^{k+i} \binom{2k}{i} (x/t)^{2k-i} \right] \quad (\text{C.10})$$

892 We identify the first term in brackets as the i -th moment of the initial distribution, which
893 we defined as the coefficients a_{i+1} in (18). We define the second term in brackets as the
894 function $\rho_i(\eta)$, where $\eta = x/t$. For $i = 0$,

$$895 \quad \rho_0(\eta) = \frac{1}{\pi} \sum_{k=0}^{\infty} (-1)^k (\eta)^{2k} = \frac{1}{\pi} \frac{1}{1 + \eta^2} \quad (\text{C.11})$$

896 where the latter equality follows from the Taylor expansion (C.5). We note that this Tay-
897 lor expansion suffers from a limited radius of convergence ($\eta^2 < 1$) owing to poles in
898 the function being expanded. Such would not be an issue, for instance, when following
899 a series of analogous steps to derive asymptotic expansions for the classical diffusion equa-
900 tion; however, we nonetheless can proceed here to derive the asymptotic expansion for
901 Hilbert diffusion.

902

903 Given the definition of ρ_i , a recursion relation follows

$$904 \quad \rho_{i+1}(\eta) = \frac{-1}{i+1} \rho'_i(\eta) \quad (\text{C.12})$$

905 Furthermore, since $\rho_0(\eta)$ is identically $\text{Re}[f_1(\eta)]$ and $f_n(\eta)$ follows the recursion relation

906 $f_{n+1}(\eta) = -f'_n(\eta)/n$, we deduce that

$$907 \quad \text{Re}[f_n(\eta)] = \rho_{n-1}(\eta) \quad \text{for } n = 1, 2, \dots \quad (\text{C.13})$$

908 such that the last bracketed term in (C.10) is seen to be the Taylor expansion of $\text{Re}[f_{i+1}(\eta)]$
909 and we may rewrite (C.10) as

$$910 \quad V(x, t) = \sum_{n=1}^{\infty} \frac{1}{t^n} a_n \text{Re}[f_n(\eta)] \quad (\text{C.14})$$

911

If the Hilbert transform of the initial distribution $V(x, 0)$ exists, there will also be complementary terms to the asymptotic expansion (C.14)

$$V(x, t) = \sum_{n=1}^{\infty} \frac{1}{t^n} a_n \operatorname{Re}[f_n(\eta)] + \sum_{n=1}^{\infty} \frac{1}{t^n} b_n \operatorname{Im}[f_n(\eta)] \quad (\text{C.15})$$

To show the existence of the latter additional terms, we would begin by repeating the procedure that lead to (C.14) but substituting $\mathcal{H}[V(x, t)]$ and $\mathcal{H}[V(x', 0)]$ for $V(x, t)$ and $V(x', 0)$ in (C.4), since $\mathcal{H}[V(x, t)]$ also satisfies the Hilbert diffusion equation and hence its solution can also be found by such a Green's function convolution. Doing so, we would arrive to an expression similar to (C.14) above

$$\mathcal{H}[V(x, t)] = \sum_{n=1}^{\infty} \frac{1}{t^n} b_n \operatorname{Re}[f_n(\eta)] \quad (\text{C.16})$$

where the coefficients b_{i+1} are identified as the i-th moment of the initial distribution of $\mathcal{H}[V(x', 0)]$. Taking the inverse Hilbert transform of (C.16) we would arrive to the second term in (C.15), after recalling that $\mathcal{H}(\operatorname{Re}[f_n(\eta)]) = -\operatorname{Im}[f_n(\eta)]$. This accounts for the complete asymptotic expansion for slip rate as given in (C.3) and (16).

925 D: Relation between conjugate harmonic functions on the real line

The Cauchy integral formula for a complex analytic function f of the complex variable w states that, for a point v on the contour C [e.g., *Carrier et al.*, 1983],

$$f(v) = -\frac{i}{\pi} \oint_C \frac{f(w)}{w-v} dw \quad (\text{D.1})$$

Take C to be the semicircular contour of radius R whose straight segment travels along the horizontal axis and whose arc lies in the upper half plane. For a function f that vanishes far from the origin, we may take $R \rightarrow \infty$ such that the contour integral reduces to an integral along the real line and

$$f(\eta, \xi = 0) = -\frac{i}{\pi} \int_{-\infty}^{\infty} \frac{f(s, r=0)}{s-\eta} ds \quad (\text{D.2})$$

where the complex numbers $v = \eta + i\xi$ and $w = s + ir$. Denote the real and imaginary parts of f as

$$f(\eta, \xi) = g(\eta, \xi) + ih(\eta, \xi) \quad (\text{D.3})$$

where g and h are the conjugate harmonic functions satisfying the Cauchy-Riemann conditions. Substituting (3) into (2),

$$g(\eta, 0) + ih(\eta, 0) = -\frac{i}{\pi} \int_{-\infty}^{\infty} \frac{g(s, 0) + ih(s, 0)}{s-\eta} ds \quad (\text{D.4})$$

940 Equating the real and imaginary parts of (4), we arrive to the relations

941
$$g = \mathcal{H}(h), \quad h = -\mathcal{H}(g) \quad (\text{D.5})$$

942 where we continue to use the shorthand $\mathcal{H}(f) = (1/\pi) \int_{-\infty}^{\infty} f(s)/(s - \eta) ds$, suppress-
943 ing explicit reference to the null imaginary parts of v and w .

944 **Acknowledgments**

945 R. C. Viesca gratefully acknowledges support as a Professeur Invité at MINES ParisTech,
946 as well as from NSF grants EAR-1653382 and 1344993, and the Southern California Earth-
947 quake Center (this is SCEC contribution 8132). SCEC is funded by NSF Cooperative
948 Agreement EAR-1033462 and USGS Cooperative Agreement G12AC20038. The presented
949 results are readily reproduced following the detailed analytical methods.

950

951 **References**

- 952 Aguiar, A. C., T. I. Melbourne, and C. W. Scrivner (2009), Moment release rate of
953 Cascadia tremor constrained by GPS, *J. Geophys. Res.*, **114**, B00A05.
- 954 Allen, C. R., M. Wyss, J. N. Brune, A. Grantz, and R. E. Wallace (1972), Displace-
955 ments on the Imperial, Superstition Hills, and San Andreas faults triggered by the
956 Borrego Mountain earthquake, in *The Borrego Mountain Earthquake of April 9,*
957 pp. 55–86, United States Geological Survey Professional Paper 787.
- 958 Ando, R., R. Nakata, and T. Hori (2010), A slip pulse model with fault heterogene-
959 ity for low-frequency earthquakes and tremor along plate interfaces, *Geophys. Res.*
960 *Lett.*, **37**, L10310.
- 961 Ando, R., N. Takeda, and T. Yamashita (2012), Propagation dynamics of seismic
962 and aseismic slip governed by fault heterogeneity and Newtonian rheology, *J.*
963 *Geophys. Res.*, **117**, B11308.
- 964 Ariyoshi, K., T. Matsuzawa, and A. Hasegawa (2007), The key frictional parameters
965 controlling spatial variations in the speed of postseismic-slip propagation on a
966 subduction plate boundary, *Earth Planet. Sc. Lett.*, **256**(1-2), 136–146.
- 967 Azúa, B. M., C. DeMets, and T. Masterlark (2002), Strong interseismic coupling,
968 fault afterslip, and viscoelastic flow before and after the Oct. 9, 1995 Colima-
969 Jalisco earthquake: Continuous GPS measurements from Colima, Mexico, *Geo-*

- 970 *phys. Res. Lett.*, 29(8), 1281.
- 971 Barbot, S., Y. Fialko, and Y. Bock (2009), Postseismic deformation due to the M_w
972 6.0 2004 Parkfield earthquake: Stress-driven creep on a fault with spatially vari-
973 able rate-and-state friction parameters, *J. Geophys. Res.*, 114, B07405.
- 974 Barenblatt, G. I. (1996), *Scaling, self-similarity, and intermediate asymptotics*, Cam-
975 bridge University Press, Cambridge.
- 976 Bar-Sinai, Y., E. A. Brener, and E. Bouchbinder (2012), Slow rupture of frictional
977 interfaces, *Geophys. Res. Lett.*, 39, L03308.
- 978 Bartlow, N. M., S. Miyazaki, A. M. Bradley, and P. Segall (2011), Space-time corre-
979 lation of slip and tremor during the 2009 Cascadia slow slip event, *Geophys. Res.*
980 Lett., 38, L18309.
- 981 Beavan, J., R. Bilham, and K. Hurst (1984), Coherent tilt signals observed in the
982 Shumagin Seismic Gap: Detection of time-dependent subduction at depth?, *J.*
983 *Geophys. Res.*, 89(B6), 4478–4492.
- 984 Bedford, J., M. Moreno, J. C. Baez, D. Lange, F. Tilmann, M. Rosenau, O. Heid-
985 bach, O. Oncken, M. Bartsch, A. Rietbrock, A. Tassara, M. Bevis, and C. Vigny
986 (2013), A high-resolution, time-variable afterslip model for the 2010 Maule $M_w =$
987 8.8, Chile megathrust earthquake, *Earth Planet. Sc. Lett.*, 383, 26–36.
- 988 Bilham, R. (1989), Surface slip subsequent to the 24 November 1987 Superstition
989 Hills, California, earthquake monitored by digital creepmeters, *B. Seismol. Soc.*
990 Am., 79(2), 424–450.
- 991 Brantut, N., and R. C. Viesca (2015), Earthquake nucleation in intact or healed
992 rocks, *J. Geophys. Res.*, 120(1), 191–209.
- 993 Brener, E. A., and V. I. Marchenko (2002), Frictional shear cracks, *J. Exp. Theor.*
994 *Phys. Lett.*, 76(4), 211–214.
- 995 Bruhat, L., S. Barbot, and J.-P. Avouac (2011), Evidence for postseismic deforma-
996 tion of the lower crust following the 2004 $M_w 6.0$ Parkfield earthquake, *J. Geophys.*
997 *Res.*, 116, B08401.
- 998 Bucknam, R. C., G. Plafker, and R. V. Sharp (1978), Fault movement (afterslip)
999 following the Guatemala earthquake of February 4, 1976, *Geology*, 6(3), 170–173.
- 1000 Bürgmann, R., M. G. Kogan, V. E. Levin, C. H. Scholz, R. W. King, and G. M.
1001 Steblow (2001), Rapid aseismic moment release following the 5 December, 1997
1002 Kronotsky, Kamchatka, Earthquake, *Geophys. Res. Lett.*, 28(7), 1331–1334.

- 1003 Cakir, Z., S. Ergintav, H. Ozener, U. Dogan, A. M. Akoglu, M. Meghraoui, and
1004 R. Reilinger (2012), Onset of aseismic creep on major strike-slip faults, *Geology*,
1005 40(12), 1115–1118.
- 1006 Carrier, G. F., and C. E. Pearson (1976), *Partial differential equations*, Academic
1007 Press, New York.
- 1008 Carrier, G. F. , M. Krook, and C. E. Pearson (1983), *Functions of a complex vari-*
1009 *able*, Hod Books, Ithaca, N.Y.
- 1010 Dascalu, C., I. R. Ionescu, and M. Campillo (2000), Fault finiteness and initiation of
1011 dynamic shear instability, *Earth Planet. Sc. Lett.*, 177(3-4), 163–176.
- 1012 de Michele, M., D. Raucoules, F. Rolandone, P. Briole, J. Salichon, A. Lemoine,
1013 and H. Aochi (2011), Spatiotemporal evolution of surface creep in the Parkfield
1014 region of the San Andreas Fault (1993–2004) from synthetic aperture radar, *Earth*
1015 *Planet. Sc. Lett.*, 308(1-2), 141–150.
- 1016 Dieterich, J. H. (1979), Modeling of Rock Friction 1. Experimental Results and
1017 Constitutive Equations, *J. Geophys. Res.*, 84(B5), 2161–2168.
- 1018 Dieterich, J. H. (1992), Earthquake nucleation on faults with rate-and state-
1019 dependent strength, *Tectonophysics*, 211(1), 115–134.
- 1020 Douglas, A., J. Beavan, L. Wallace, and J. Townend (2005), Slow slip on the north-
1021 ern Hikurangi subduction interface, New Zealand, *Geophys. Res. Lett.*, 32(16),
1022 3–4.
- 1023 Dragert, H., K. Wang, and T. S. James (2001), A Silent Slip Event on the Deeper
1024 Cascadia Subduction Interface, *Science*, 292(5521), 1525–1528.
- 1025 Evans, K. F., R. O. Burford, and G. C. P. King (1981), Propagating episodic creep
1026 and the aseismic slip behavior of the Calaveras Fault north of Hollister, California,
1027 *J. Geophys. Res.*, 86(B5), 3721–3735.
- 1028 Freed, A. M. (2007), Afterslip (and only afterslip) following the 2004 Parkfield,
1029 California, earthquake, *Geophys. Res. Lett.*, 34, L06312.
- 1030 Fu, Y., and J. T. Freymueller (2013), Repeated large Slow Slip Events at the south-
1031 central Alaska subduction zone, *Earth Planet. Sc. Lett.*, 375, 303–311.
- 1032 Gao, H., D. A. Schmidt, and R. J. Weldon (2012), Scaling Relationships of Source
1033 Parameters for Slow Slip Events, *B. Seismol. Soc. Am.*, 102(1), 352–360.
- 1034 Garagash, D. I. (2012), Seismic and aseismic slip pulses driven by thermal pressur-
1035 ization of pore fluid, *J. Geophys. Res.*, 117, B04314.

- 1036 Gladwin, M. T., R. L. Gwyther, R. H. G. Hart, and K. S. Breckenridge (1994),
1037 Measurements of the strain field associated with episodic creep events on the
1038 San Andreas Fault at San Juan Bautista, California, *J. Geophys. Res.*, **99**(B3),
1039 4559–4565.
- 1040 Gomberg, J., J. L. Rubinstein, Z. Peng, K. C. Creager, J. E. Vidale, and P. Bodin
1041 (2008), Widespread triggering of nonvolcanic tremor in California, *Science*,
1042 **319**(5860), 173.
- 1043 Gu, J.-C., J. R. Rice, A. L. Ruina, and S. T. Tse (1984), Slip motion and stability of
1044 a single degree of freedom elastic system with rate and state dependent friction, *J.*
1045 *Mech. Phys. Solids*, **32**(3), 167–196.
- 1046 Guilhem, A., and R. M. Nadeau (2012), Episodic tremors and deep slow-slip events
1047 in Central California, *Earth Planet. Sc. Lett.*, **357**–**358**, 1–10.
- 1048 Hashimoto, M., N. Choosakul, M. Hashizume, S. Takemoto, H. Takiguchi,
1049 Y. Fukuda, and K. Fujimori (2006), Crustal deformations associated with the
1050 great Sumatra-Andaman earthquake deduced from continuous GPS observation,
1051 *Earth, Planets and Space*, **58**(2), 127–139.
- 1052 Hearn, E. H. (2002), Dynamics of Izmit Earthquake Postseismic Deformation and
1053 Loading of the Duzce Earthquake Hypocenter, *B. Seismol. Soc. Am.*, **92**(1), 172–
1054 193.
- 1055 Heki, K., S. Miyazaki, and H. Tsuji (1997), Silent fault slip following an interplate
1056 thrust earthquake at the Japan Trench, *Nature*, **386**(6625), 595–598.
- 1057 Helmstetter, A., and B. E. Shaw (2009), Afterslip and aftershocks in the rate-and-
1058 state friction law, *J. Geophys. Res.*, **114**, B01,308.
- 1059 Hetland, E. A., M. Simons, and E. M. Dunham (2010), Post-seismic and interseismic
1060 fault creep I: model description, *Geophys. J. Int.*, **181**(1), 81–98.
- 1061 Hirose, H., and K. Obara (2005), Repeating short- and long-term slow slip events
1062 with deep tremor activity around the Bungo channel region, southwest Japan,
1063 *Earth, Planets and Space*, **57**(10), 961–972.
- 1064 Hirose, H., K. Hirahara, F. Kimata, N. Fujii, and S. Miyazaki (1999), A slow thrust
1065 slip event following the two 1996 Hyuganada Earthquakes beneath the Bungo
1066 Channel, southwest Japan, *Geophys. Res. Lett.*, **26**(21), 3237–3240.
- 1067 Hirose, H., T. Matsuzawa, T. Kimura, and H. Kimura (2014), The Boso slow slip
1068 events in 2007 and 2011 as a driving process for the accompanying earthquake

- 1069 swarm, *Geophys. Res. Lett.*, 41(8), 2778–2785.
- 1070 Hsu, Y.-J. (2006), Frictional Afterslip Following the 2005 Nias-Simeulue Earthquake,
1071 Sumatra, *Science*, 312(5782), 1921–1926.
- 1072 Hsu, Y.-J., N. Bechor, P. Segall, S.-B. Yu, L.-C. Kuo, and K.-F. Ma (2002), Rapid
1073 afterslip following the 1999 Chi-Chi, Taiwan Earthquake, *Geophys. Res. Lett.*,
1074 29(16), 1–4.
- 1075 Hsu, Y.-J., P. Segall, S.-B. Yu, L.-C. Kuo, and C. A. Williams (2007), Temporal and
1076 spatial variations of post-seismic deformation following the 1999 Chi-Chi, Taiwan
1077 earthquake, *Geophys. J. Int.*, 169(2), 367–379.
- 1078 Ida, Y. (1974), Slow-moving deformation pulses along tectonic faults, *Phys. Earth*
1079 *Planet. In.*, 9(4), 328–337.
- 1080 Ide, S., G. C. Beroza, D. R. Shelly, and T. Uchide (2007a), A scaling law for slow
1081 earthquakes, *Nature*, 447(7140), 76–79.
- 1082 Ide, S., D. R. Shelly, and G. C. Beroza (2007b), Mechanism of deep low frequency
1083 earthquakes: Further evidence that deep non-volcanic tremor is generated by
1084 shear slip on the plate interface, *Geophys. Res. Lett.*, 34(3), 2191–5.
- 1085 Ito, Y., K. Obara, K. Shiomi, S. Sekine, and H. Hirose (2007), Slow Earthquakes
1086 Coincident with Episodic Tremors and Slow Slip Events, *Science*, 315(5811),
1087 503–506.
- 1088 Johnson, K. M., R. Bürgmann, and K. Larson (2006), Frictional Properties on the
1089 San Andreas Fault near Parkfield, California, Inferred from Models of Afterslip
1090 following the 2004 Earthquake, *B. Seismol. Soc. Am.*, 96(4B), S321–S338.
- 1091 Johnson, K. M., R. Bürgmann, and J. T. Freymueller (2009), Coupled afterslip and
1092 viscoelastic flow following the 2002 Denali Fault, Alaska earthquake, *Geophys. J.*
1093 *Int.*, 176(3), 670–682.
- 1094 Jolivet, R., C. Lasserre, M. P. Doin, G. Peltzer, J. P. Avouac, J. Sun, and R. Dailu
1095 (2013), Spatio-temporal evolution of aseismic slip along the Haiyuan fault, China:
1096 Implications for fault frictional properties, *Earth Planet. Sc. Lett.*, 377–378, 23–33.
- 1097 Kostoglodov, V., S. K. Singh, J. A. Santiago, S. I. Franco, K. M. Larson, A. R.
1098 Lowry, and R. Bilham (2003), A large silent earthquake in the Guerrero seismic
1099 gap, Mexico, *Geophys. Res. Lett.*, 30(15), 1807.
- 1100 Li, D., and Y. Liu (2016), Spatiotemporal evolution of slow slip events in a nonpla-
1101 nar fault model for northern Cascadia subduction zone, *J. Geophys. Res.*, 121(9),

- 1102 6828–6845.
- 1103 Linde, A. T., M. T. Gladwin, M. J. S. Johnston, R. L. Gwyther, and R. G. Bilham
1104 (1996), A slow earthquake sequence on the San Andreas fault, *Nature*, 383(6595),
1105 65–68.
- 1106 Linker, M. F., and J. R. Rice (1997), Models of postseismic deformation and stress
1107 transfer associated with the Loma Prieta earthquake , in *The Loma Prieta, California, Earthquake of October 17, 1989: Aftershocks and Postseismic Effects*,
1108 United States Geological Survey Professional Paper 1550D.
- 1109 Liu, Y. (2014), Source scaling relations and along-strike segmentation of slow slip
1110 events in a 3-D subduction fault model, *J. Geophys. Res.*, 119(8), 6512–6533.
- 1111 Liu, Y., and J. R. Rice (2005), Aseismic slip transients emerge spontaneously in
1112 three-dimensional rate and state modeling of subduction earthquake sequences, *J.
1113 Geophys. Res.*, 110, B08307.
- 1114 Liu, Y., and J. R. Rice (2007), Spontaneous and triggered aseismic deformation
1115 transients in a subduction fault model, *J. Geophys. Res.*, 112, B09,404.
- 1116 Lowry, A. R., K. M. Larson, V. Kostoglodov, and R. Bilham (2001), Transient fault
1117 slip in Guerrero, southern Mexico, *Geophys. Res. Lett.*, 28(19), 3753–3756.
- 1118 Marone, C. J., C. H. Scholtz, and R. Bilham (1991), On the mechanics of earth-
1119 quake afterslip, *J. Geophys. Res.*, 96(B5), 8441–8452.
- 1120 Miller, M. M. (2002), Periodic Slow Earthquakes from the Cascadia Subduction
1121 Zone, *Science*, 295(5564), 2423–2423.
- 1122 Montési, L. G. J. (2004), Controls of shear zone rheology and tectonic loading on
1123 postseismic creep, *J. Geophys. Res.*, 109, B10,404.
- 1124 Murray, J., and J. Langbein (2006), Slip on the San Andreas Fault at Parkfield, Cal-
1125 ifornia, over Two Earthquake Cycles, and the Implications for Seismic Hazard, *B.
1126 Seismol. Soc. Am.*, 96(4B), S283–S303.
- 1127 Murray, J. R., and P. Segall (2005), Spatiotemporal evolution of a transient slip
1128 event on the San Andreas fault near Parkfield, California, *J. Geophys. Res.*, 110,
1129 B09,407.
- 1130 Nadeau, R. M., and D. Dolenc (2005), Nonvolcanic Tremors Deep Beneath the San
1131 Andreas Fault, *Science*, 307(5708), 389–389.
- 1132 Nason, R., and J. Weertman (1973), A dislocation theory analysis of fault creep
1133 events, *J. Geophys. Res.*, 78(32), 7745–7751.
- 1134

- 1135 Obara, K. (2002), Nonvolcanic Deep Tremor Associated with Subduction in South-
1136 west Japan, *Science*, 296(5573), 1679–1681.
- 1137 Obara, K., and H. Hirose (2006), Non-volcanic deep low-frequency tremors ac-
1138 companying slow slips in the southwest Japan subduction zone, *Tectonophysics*,
1139 417(1-2), 33–51.
- 1140 Obara, K., H. Hirose, F. Yamamizu, and K. Kasahara (2004), Episodic slow slip
1141 events accompanied by non-volcanic tremors in southwest Japan subduction zone,
1142 *Geophys. Res. Lett.*, 31, L23,602.
- 1143 Ohta, Y., J. Freymueller, S. Hreinsdottir, and H. Suito (2006), A large slow slip
1144 event and the depth of the seismogenic zone in the south central Alaska subduc-
1145 tion zone, *Earth Planet. Sc. Lett.*, 247(1-2), 108–116.
- 1146 Outerbridge, K. C., T. H. Dixon, S. Y. Schwartz, J. I. Walter, M. Protti, V. Gon-
1147 zalez, J. Biggs, M. Thorwart, and W. Rabbel (2010), A tremor and slip event on
1148 the Cocos-Caribbean subduction zone as measured by a global positioning system
1149 (GPS) and seismic network on the Nicoya Peninsula, Costa Rica, *J. Geophys.
1150 Res.*, 115, B10408.
- 1151 Ozawa, S., T. Nishimura, H. Suito, T. Kobayashi, M. Tobita, and T. Imakiire
1152 (2011), Coseismic and postseismic slip of the 2011 magnitude-9 Tohoku-Oki earth-
1153 quake, *Nature*, 475(7356), 373–376.
- 1154 Ozawa, S., T. Nishimura, H. Munekane, H. Suito, T. Kobayashi, M. Tobita, and
1155 T. Imakiire (2012), Preceding, coseismic, and postseismic slips of the 2011 Tohoku
1156 earthquake, Japan, *J. Geophys. Res.*, 117, B07404.
- 1157 Paul, J., A. R. Lowry, R. Bilham, S. Sen, and R. Smalley Jr. (2007), Postseismic
1158 deformation of the Andaman Islands following the 26 December, 2004 Great
1159 Sumatra–Andaman earthquake, *Geophys. Res. Lett.*, 34, L19309.
- 1160 Perfettini, H., and J. P. Avouac (2004), Postseismic relaxation driven by brittle
1161 creep: A possible mechanism to reconcile geodetic measurements and the decay
1162 rate of aftershocks, application to the Chi-Chi earthquake, Taiwan, *J. Geophys.
1163 Res.*, 109, B02304.
- 1164 Perfettini, H., J.-P. Avouac, H. Tavera, A. Kositsky, J.-M. Nocquet, F. Bondoux,
1165 M. Chlieh, A. Sladen, L. Audin, D. L. Farber, and P. Soler (2010), Detailed imag-
1166 ing of the 2007 Pisco co-seismic and post-seismic deformation - implications on
1167 the seismogenic behavior of subduction megathrusts, *Nature*, 465(7294), 78–81.

- 1168 Perrin, G., J. R. Rice, and G. Zheng (1995), Self-healing slip pulse on a frictional
1169 surface, *J. Mech. Phys. Solids*, *43*(9), 1461–1495.
- 1170 Putelat, T., J. H. P. Dawes, and A. R. Champneys (2017), A phase-plane analysis of
1171 localized frictional waves, *Proc. Roy. Soc. A*, *473*, 20160606.
- 1172 Ranjith, K., and J. R. Rice (1999), Stability of quasi-static slip in a single degree
1173 of freedom elastic system with rate and state dependent friction, *J. Mech. Phys.
1174 Solids*, *47*(6), 1207–1218.
- 1175 Reilinger, R. E., S. Ergintav, R. Bürgmann, S. McClusky, O. Lenk, A. Barka,
1176 O. Gurkan, L. Hearn, K. L. Feigl, R. Cakmak, B. Aktug, H. Ozener, and M. N.
1177 Toksoz (2000), Coseismic and Postseismic Fault Slip for the 17 August 1999, M =
1178 7.5, Izmit, Turkey Earthquake, *Science*, *289*(5484), 1519–1524.
- 1179 Rice, J. R., and A. L. Ruina (1983), Stability of steady frictional slipping, *J. Appl.
1180 Mech.*, *50*, 343–349.
- 1181 Rice, J. R., and S. T. Tse (1986), Dynamic motion of a single degree of freedom sys-
1182 tem following a rate and state dependent friction law, *J. Geophys. Res.*, *91*(B1),
1183 521–530.
- 1184 Rice, J. R., N. Lapusta, and K. Ranjith (2001), Rate and state dependent friction
1185 and the stability of sliding between elastically deformable solids, *J. Mech. Phys.
1186 Solids*, *49*(9), 1865–1898.
- 1187 Rogers, G., and H. Dragert (2003), Episodic Tremor and Slip on the Cascadia Sub-
1188duction Zone: The Chatter of Silent Slip, *Science*, *300*(5627), 1942–1943.
- 1189 Romanet, P., H. S. Bhat, R. Jolivet, and R. Madariaga (2018), Fast and Slow Slip
1190 Events Emerge Due to Fault Geometrical Complexity, *Geophys. Res. Lett.*, *45*(10),
1191 4809–4819.
- 1192 Rousset, B., R. Jolivet, M. Simons, C. Lasserre, B. Riel, P. Milillo, Z. Çakir, and
1193 F. Renard (2016), An aseismic slip transient on the North Anatolian Fault, *Geo-
1194 phys. Res. Lett.*, *43*(7), 3254–3262.
- 1195 Rubin, A. M. (2008), Episodic slow slip events and rate-and-state friction, *J. Geo-
1196 phys. Res.*, *113*, B11414.
- 1197 Rubinstein, J. L., J. E. Vidale, J. Gomberg, P. Bodin, K. C. Creager, and S. D. Mal-
1198 one (2007), Non-volcanic tremor driven by large transient shear stresses, *Nature*,
1199 *448*(7153), 579–582.

- 1200 Ruina, A. (1983), Slip instability and state variable friction laws, *88*(B12), 10,359–
1201 10–370.
- 1202 Ruina, A. L. (1980), Friction laws and instabilities: A quasistatic analysis of some
1203 dry frictional behavior., Ph.D. thesis, Brown University.
- 1204 Savage, J. C. (1971), A Theory of Creep Waves propagating along a transform fault,
1205 *J. Geophys. Res.*, *76*(8), 1954–1966.
- 1206 Savage, J. C., and J. L. Svart (1997), Postseismic deformation associated with
1207 the 1992 Mw = 7.3 Landers earthquake, southern California, *J. Geophys. Res.*,
1208 *102*(B4), 7565–7577.
- 1209 Scholz, C. H. (1990), *The Mechanics of Earthquakes and Faulting*, Cambridge Uni-
1210 versity Press, Cambridge.
- 1211 Scholz, C. H., M. Wyss, and S. W. Smith (1969), Seismic and aseismic slip on the
1212 San Andreas Fault, *J. Geophys. Res.*, *74*(8), 2049–2069.
- 1213 Schwartz, S. Y., and J. M. Rokosky (2007), Slow slip events and seismic tremor at
1214 circum-Pacific subduction zones, *Rev. Geophys.*, *45*(3), RG3004.
- 1215 Segall, P. (2010), *Earthquake and Volcano Deformation*, Princeton University Press,
1216 Princeton.
- 1217 Segall, P., A. M. Rubin, A. M. Bradley, and J. R. Rice (2010), Dilatant strengthen-
1218 ing as a mechanism for slow slip events, *J. Geophys. Res.*, *115*, B12305.
- 1219 Shelly, D. R., and K. M. Johnson (2011), Tremor reveals stress shadowing, deep
1220 postseismic creep, and depth-dependent slip recurrence on the lower-crustal San
1221 Andreas fault near Parkfield, *Geophys. Res. Lett.*, *38*, L13312.
- 1222 Shelly, D. R., G. C. Beroza, S. Ide, and S. Nakamura (2006), Low-frequency earth-
1223 quakes in Shikoku, Japan, and their relationship to episodic tremor and slip,
1224 *Nature*, *442*(7099), 188–191.
- 1225 Shen, Z. K., D. D. Jackson, Y. Feng, M. Cline, M. Kim, P. Fang, and Y. Bock (),
1226 Postseismic deformation following the Landers earthquake, California, 28 June
1227 1992, *B. Seismol. Soc. Am.*, *84*(3), 780–791.
- 1228 Shibazaki, B., K. Obara, T. Matsuzawa, and H. Hirose (2012), Modeling of slow slip
1229 events along the deep subduction zone in the Kii Peninsula and Tokai regions,
1230 southwest Japan, *J. Geophys. Res.*, *117*, B06,311.
- 1231 Shirzaei, M., and R. Bürgmann (2013), Time-dependent model of creep on the Hay-
1232 ward fault from joint inversion of 18?years of InSAR and surface creep data, *J.*

- 1233 *Geophys. Res.*, 118(4), 1733–1746.
- 1234 Skarbek, R. M., A. W. Rempel, and D. A. Schmidt (2012), Geologic heterogeneity
1235 can produce aseismic slip transients, *Geophys. Res. Lett.*, 39, L21306.
- 1236 Smith, S. W., and M. Wyss (1968), Displacement on the San Andreas fault subse-
1237 quent to the 1966 Parkfield earthquake, *B. Seismol. Soc. Am.*, 58(6), 1955–1973.
- 1238 Steinbrugge, K. V., E. G. Zacher, D. Tocher, C. A. Whitten, and C. N. Claire
1239 (1960), Creep on the San Andreas fault, *B. Seismol. Soc. Am.*, 50(3), 389–415.
- 1240 Uenishi, K., and J. R. Rice (2003), Universal nucleation length for slip-weakening
1241 rupture instability under nonuniform fault loading, *J. Geophys. Res.*, 108(B1),
1242 2042.
- 1243 Viesca, R. C. (2016), Stable and unstable development of an interfacial sliding insta-
1244 bility, *Phys. Rev. E*, 93(6), 060202(R).
- 1245 Wallace, L. M., and J. Beavan (2006), A large slow slip event on the central Hiku-
1246 rangi subduction interface beneath the Manawatu region, North Island, New
1247 Zealand, *Geophys. Res. Lett.*, 33, L11301.
- 1248 Wech, A. G., C. M. Boese, T. A. Stern, and J. Townend (2012), Tectonic tremor and
1249 deep slow slip on the Alpine Fault, *Geophys. Res. Lett.*, 39, L10303.
- 1250 Wesson, R. L. (1988), Dynamics of fault creep, *J. Geophys. Res.*, 93(B8), 8929–8951.
- 1251 Williams, P. L., S. F. McGill, K. E. Sieh, C. R. Allen, and J. N. Louie (1988), Trig-
1252 gered slip along the San Andreas fault after the 8 July 1986 North Palm Springs
1253 earthquake, *B. Seismol. Soc. Am.*, 78(3), 1112–1122.
- 1254 Yu, S.-B., Y.-J. Hsu, L.-C. Kuo, H.-Y. Chen, and C.-C. Liu (2003), GPS measure-
1255 ment of postseismic deformation following the 1999 Chi-Chi, Taiwan, earthquake,
1256 *J. Geophys. Res.*, 108(B11), 2520.